SPACE SCIENCES LABORATORY

SCIENTIFIC RATIONALE FOR APOLLO LUNAR (ORBITAL) ELECTROMAGNETIC SOUNDER EXPERIMENT

By Stanley H. Ward

Final Technical Report on
NASA Contract NAS 2-4996, Item 277

Space Sciences Laboratory Series 11, Issue 22

March 1970

UNIVERSITY OF CALIFORNIA, BERKELEY

Space Sciences Laboratory
University of California
Berkeley, California

SCIENTIFIC RATIONALE FOR APOLLO LUNAR (ORBITAL) ELECTROMAGNETIC SOUNDER EXPERIMENT

By Stanley H. Ward

Final Technical Report on NASA Contract NAS 2-4996

Item 277

March 1970

Space Sciences Laboratory Series 11, Issue 22

SCIENTIFIC RATIONALE

FOR

APOLLO LUNAR (ORBITAL) ELECTROMAGNETIC SOUNDER EXPERIMENT

Section | Contents | Page

Section Contents Page

Section | Contents | Page

Section | Contents | Page

Section | Contents | Page

Section | Contents | Page

Preface

Item 277 of Contract NAS 2-4996 called for a *Preliminary Study of Antennas for Orbital Lunar Electromagnetic Experiment*. Technical reporting on this contract has been purposely delayed so that enlargement of the scope of Item 277 could be made. The present report, then, embodies the original assignment plus a considerable extension so that it now truly becomes a report on the Scientific Rationale of the Apollo (Orbital) Lunar Electromagnetic Sounder experiment. Without question, this report represents only the current iteration of development of this rationale.

SCIENTIFIC RATIONALE FOR
APOLLO LUNAR (ORBITAL) ELECTROMAGNETIC SOUNDER EXPERIMENT

By

Stanley H. Ward

1. Brief Description of Lunar Electromagnetic Sounder Experiment

A Lunar Electromagnetic Sounder experiment is tentatively scheduled to be part of the science payload in the mission of Apollo 19. In basic concept, the experiment requires transmission of electromagnetic waves from the spacecraft in orbit, reflection of these waves from the moon, and subsequent reception of the waves at the spacecraft. The complex ratio of received signal to transmitted signal provides information which may be interpreted in terms of the three-dimensional distributions of electrical conductivity, dielectric constant, and magnetic permeability in the lunar interior.

For purposes of illustration, it is assumed that a center-fed electric dipole antenna, mounted in Sector 1 of the Service Module of the Apollo spacecraft (Figures 1 and 2) transmits sinusoidal electromagnetic waves in square pulses at a pulse repetition rate of n per second. The outgoing electromagnetic wave is reflected from the lunar surface, and possibly from the plasma above or interfaces beneath the lunar surface; the reflected wave is monitored by the antenna used in "receive" mode. If the shape, amplitude, or time of arrival of the received pulse is known relative to the shape, amplitude, or time of transmittion of the transmitted pulse, then information on the electrical parameters to depths of order 10 km within the moon can be obtained and the particle content of any assumed lunar ionosphere might be obtained also.

2. Objectives of the Lunar Electromagnetic Sounder Experiment

2.1 Objectives re the Lunar Interior

The fundamental scientific objective is an electromagnetic sounding of the moon to depths of order 10 km to provide information on the surface

and depth distributions of the following geological parameters: (a) mineralogical and chemical composition, (b) interstitial water distribution, and (c) density. Thus, any known, inferred, or postulated layering within the moon, such as the debris layer, permafrost layer, mare bottom contacts and differentiated layers, as well as gross lateral changes associated with known, inferred, or postulated volcanism, igneous intrusion, mare-highlands contacts, meteorite impacts, mascons, "permafrost" accumulations, etc., may be evident from the data obtained with the experiment.

2.1.1 Detection of Layering

Discrete layers, if they exist beneath the lunar surface, will be measured. The details of layering will be evident from the data, as is the case for earth measurements employing EM techniques.

Major layering within the moon, such as the known debris layer, postulated ice layer, or differentiated layers, may be identified from the EM profiling. The layering need not be regular and plane-parallel for detection; the irregular buried surface of glaciers in Antarctica has been mapped by terrestrial airborne radar (see later reference).

2.1.2 Detection of Gross Inhomogeneities

Gross lateral electrical property changes which arise in volcanism, igneous intrusions, meteorite impact, "permafrost" accumulations, etc., and which possibly will be associated with mascons, mare-highland contacts, and other major geologic contacts should be evident from the EM response. These changes may result from either endogenic or exogenic sources.

2.1.3 Detection of Conductive Materials

The presence of conductive iron, iron oxides, or other metallic minerals is expected to give characteristic EM response.

2.1.4 Detection of Mascons

The presence of shallow mascons in the vicinity of an EM Sounder orbit may be evident in the sounder data. The composition of the mascons, i.e., whether they are dense basaltic phases, or meteorites rich in iron or iron oxides will determine the nature of the EM response.

Possibly the details of the response will indicate the size, location, and/or the composition of the mascons.

2.1.5 Detection of Lunar Subsurface Water

The presence of subsurface water is evident in characteristic "signatures" obtained in theoretical studies of elementary models of the moon. Absence of these characteristic signatures implies a dry lunar subsurface.

Presence of water (in pore liquid or permafrost form) can be identified, for amounts greater than a fraction of 1 percent, if the water is ionized. The results from Apollo 11 might be interpreted as discouraging re this objective, but the evidence is by no means conclusive.

2.1.6 Technological Objectives

The specific technological objectives that lead to the scientific objectives stated above are spatial maps of conductivity, dielectric constant, and other electromagnetic parameters (e.g., reflection coefficient, pulse shape) over the lunar surface as functions of time and/or frequency and/or polarization.

The ability to realize the scientific objectives then depends on (a) resolution, which in turn depends on wavelength, antenna pattern, and spacecraft height (b) presence of physical property (electromagnetic parameter) contrasts, and (c) ability to correlate the rock and water forms to the electromagnetic parameters.

2.2 Objectives re the Lunar Environment

2.2.1 General

These objectives are secondary to those concerning the lunar interior. Detection and characterization of a possible lunar ionosphere is, however, a meaningful objective of the proposed experiment. Knowledge of the existence of a lunar ionosphere would be fundamental to an understanding of the interaction between the moon and the solar wind and radiation incident upon it. Measurement of the sheath of charge on the sunlight side of the moon is also of interest for the same reason. There is no guarantee that either an ionosphere or a sheath exists or can be detected,

however, as subsequent discussion will reveal. Hence, their detection must be treated as secondary to the lunar interior objectives. Specifically, the environmental objectives are as follows.

2.2.2 Detection of a Lunar Ionosphere

The hypothetical lunar ionosphere, if it has a density of electrons greater than 100 per cubic centimeter, will be sounded, provided that the reflecting horizon is at a distance from the spacecraft greater than approximately $c\tau/2$, where c is the speed of light and τ is the pulse length. A density of 10^6 electrons per cubic centimeter represents the upper limit to the expected density (as in the case of th earth's ionosphere), although a density this high is not probab .

2.2.3 Detection of the Lunar Surface Plasma Sheath

A sheath of charged particles may occur on the sunlit surface of the moon. Depending on its density and extent, this sheath could contribute to the reflected EM wave, and thereby be measured — although this seems doubtful (see later discussion).

2.3 Other Possible Applications for this Facility

The following possible applications are listed because of related interests, but are not basic objectives of the proposed experiment. One can look upon them as added benefits of the experiment.

2.3.1 Measurement of Solar Wind EM Noise

Measurements during programmed transmitter-off intervals will yield values for EM noise caused by solar wind interaction with the moon, as well as for natural plasma oscillations within the solar wind. These measurements will be related to the spacecraft position relative to the sun. When the spacecraft is shielded from the sun by appreciable lunar mass, solar wind EM noise may be absent.

2.3.2 Measurement of Cosmic Noise

A passive measurement during programmed transmitter-off intervals will yield values for EM noise of cosmic origin. These measurements will be related to the spacecraft position relative to the sun, earth, and other planets.

2.3.3 Measurement of Earth Transmissions

Measurements during programmed transmitter-off intervals may yield values for EM earth transmission in the frequency range above earth ionosphere cutoff. Bistatic measurements of lunar subsurface electrical parameters then become possible.

2.3.4 Earth Receptions of Field Transmitted by Lunar Electromagnetic Sounder

At frequencies above the earth ionosphere cutoff, reception on the earth of transmitted Lunar EM Sounder signals may be possible. If so, bistatic measurement of lunar subsurface electrical parameters will then be possible.

2.3.5 Lunar Spherical Lens Experiment

Salisbury (1967) has proposed that the diffraction of electromagnetic waves in the 10^4 Hz to 10^8 Hz band by the moon will be such that the field of an earth-based transmitter will be focused behind the moon. If such a phenomenon does occur, then it will be monitored by the Lunar Electromagnetic Sounder during intervals when the Sounder transmitter is off. This is an up-link version of an experiment which has been tried unsuccessfully down-link. Except for ionospheric effects, the radio-frequency transmissions from satellites as monitored on earth by personnel from Stanford University have demonstrated that the moon completely blocks radiofrequency transmission. Thus, while the outlook for success seems dim, the spherical lens experiment of Salisbury can be carried out both up-link and down-link once the Lunar Electromagnetic Sounder is placed in lunar orbit.

2.3.6 Development for Future Lunar and Planetary EM Experiments

Experience gained with the Lunar Electromagnetic Sounder would be invaluable in designing EM systems for such important missions as the orbital detection of water on or below the Martian surface, for presence of a Martian ionosphere, the mapping of major geologic units of Venus, and topside sounding of Jupiter.

3. Description of the Lunar Electromagnetic Scattering Problem

3.1 General

Backscattering of an angular spectrum of electromagnetic waves incident on the moon may be considered to consist of true specular reflection from the mean surface, by quasi-specular reflection from rough surfaces of dimensions large relative to a wavelength, and by scattering from discrete objects whose dimensions are of the order of a wavelength or less. Parameters entering into the scattering problem include:

1. the antenna configuration
2. the plasma surrounding the antenna
3. the possible lunar ionosphere and lunar plasma sheath
4. the height of the antenna above the lunar surface
5. scattering from the rough lunar surface
6. scattering from buried interfaces, which may be rough
7. scattering from buried inhomogeneities
8. the frequency range of the transmitted field
9. the polarization of the transmitted field
10. the polarization of the received field
11. the location of the receiving system relative to the transmitting system
12. the dispersion spectra of the electrical properties of the lunar materials
13. the Doppler shift of off-vertical reflections.

We shall discuss each of these parameters in the following paragraphs. The inter-relation of one parameter to another in this list will become evident.

3.2 The Antenna Configuration

Both astatic and bistatic configurations have been studied, the various versions of each being discussed below.

1. Center-fed horizontal electric dipoles are to be used for both transmission and reception. One antenna, 240 feet tip-to-tip, will cover the frequency band 10^5 Hz to 5×10^6 Hz and one

antenna, 61.5 feet tip-to-tip, will cover the frequency band 5×10^6 Hz to 2×10^7 Hz. A linearly polarized field is transmitted, while in general an elliptically polarized field is reflected from the lunar surface. Only the component of the elliptically polarized field in the direction of the axis of the antenna will be monitored with this antenna configuration. The 240-foot antenna is oriented with its axis parallel to the spacecraft axis and tangential to the orbit. The 61.5-foot antenna is oriented with its axis normal to the spacecraft axis but also tangential to the orbit.

A possible interpretational difficulty arises with this flight-rated configuration insofar as use is made of one polarization for the lower half of the band, and an orthogonal polarization for the upper half of the band.

2. The first generalization of the electric dipole configuration described above is transmission on one antenna and reception on two orthogonal antennas. If, for example, both antennas were made a nominal 60-feet long and one was used for transmission over the frequency band 10^5 Hz to 2×10^7 Hz while both were used for reception over the same frequency band, then measurements of both horizontal components of the ellipse of polarization could be made. This feature adds one more useful parameter for interpretation of resulting data. The assumption made herein is that the 60-foot antenna would have adequate gain over the whole bandwidth from 10^5 Hz to 2×10^7 Hz and this needs evaluation by a detailed study to be described later. Further, the relative phase of the two components, in addition their amplitudes, must be measured.

3. The next generalization of the electric dipole configuration is transmission on one orthogonal pair of dipoles mounted on the Service Module and reception on a second orthogonal pair of dipoles mounted on a subsatellite. Both antennas on the Service Module, being of equal size of about 60 feet tip-to-tip, would be used in alternate cycles for transmission. The orthogonal subsatellite receiving antennas, also 60 feet in length, would record the two components of the horizontal ellipse of polarization. The angle

subtended between the subsatellite and the Service Module is variable, and hence, the angle of incidence of the transmitted field is an additional variable. Again the assumption is made that the 60-foot antennas would have adequate gain over the whole bandwidth from 10^5 Hz to 2×10^7 Hz. This configuration and the next one were not considered further, once it became known that a subsatellite of ISIS A dimensions would not be available for the Apollo program.

4. An alternate form of this latter configuration would see one 240-foot and one 61.5-foot antenna at the Service Module and also at the subsatellite. Again, opposite polarizations are used for each half of the frequency band and this may lead to interpretational difficulties because of a possible discontinuity in reflected energy at the point of switching from one antenna set to the other.

5. One or more magnetic dipole or loop antennas could be used in transmission and reception. Loop diameters perhaps as large as 100 feet, or even 1,000 feet would be required to obtain adequate moment. These loops are not as efficient for far field radiation as are the electric dipoles in the passband considered. A single loop mounted on the CSM would be mechanically more unstable than the electric dipole. If this configuration is generalized to use a pair of orthogonal mechanically locked loops, then mechanical stability can be achieved. However, since loop antennas have not been used in experiments of this nature and since they do seem to pose electrical and mechanical design problems, we shall treat them no further herein.

The final antenna configuration recommended for the Lunar Electromagnetic Sounder experiment is an astatic configuration consisting of a pair of center-fed electric dipoles, two versions of which were described under items 1) and 2) above. A detailed examination of the gain, radiation pattern, and input impedance as functions of frequency for various antenna lengths is required before an optimum center-fed electric dipole configuration can be selected. Interrelated to this detailed electrical analysis is a mechanical analysis of the antennas. Static thermal deflection,

thermal flutter, torsional flexures, mechanical oscillations, plus couplings between these deflections all require evaluation for the several lengths of antennas proposed. To ensure a mechanically stable antenna, a compromise antenna length may need to be selected, and this in turn will affect the antenna electrical characteristics.

The antenna electrical characteristics will be affected by the presence of the spacecraft. This fact must be introduced into calculations, as will be described subsequently.

The antenna mechanical stability is dependent upon the several modes of spacecraft dynamic behaviour; a proposed study of this problem will be described briefly later in the report.

3.3 The Antenna Field Patterns

The configuration of the field transmitted by a center-fed linear electric dipole antenna is a function of wavelength. This wavelength dependency of field pattern is illustrated in the rough conceptual sketches of Figures 3 and 4 for the nominal 240-foot (low-band) dipole and the nominal 61.5-foot (high-band) dipole employed on the ISIS A Sounder.

Clearly, the sampling area is smaller at 2×10^7 Hz than at 5×10^6 Hz for the high-band dipole and is smaller at 5×10^6 Hz than at 10^5 Hz for the low-band dipole. Reflection from the lunar surface is therefore expected to be a function of frequency on this account alone, and hence precise knowledge of antenna field patterns is a highly desirable aspect of the experiment. It has been recommended that this information be obtained by a detailed study that takes into account the effect of the spacecraft as well as of the real antenna length.

3.4 The Plasma Surrounding the Antenna

3.4.1 The Plasma Parameters

The mean parameters of the uninterrupted solar wind are as follows:

electron density	10/cc
electron temperature	10^5 °K
interplanetary field	5 γ

electron plasma frequency	2.8×10^4 Hz
proton plasma frequency	6.6×10^2 Hz
electron gyro frequency	1.40×10^2 Hz
proton gyro frequency	0.076 Hz
velocity	400 km/sec.

The solar plasma is a fully ionized, collision-free supersonic stream of high electrical conductivity which serves as a compressible anisotropic dielectric for electromagnetic waves propagating within it.

The plasma "void" occurring on the anti-solar side of the moon exhibits much lower number densities than the uninterrupted free plasma stream. Thus, the electron and proton plasma frequencies are much lower on the anti-solar side than on the solar side of the moon.

3.4.2 The Solar Plasma as a Noise Generator

The transient behavior of the solar plasma density and magnetic field, the collisions of solar particles with the lunar surface, and the gyration of the protons and electrons about the field lines all produce electromagnetic radiation, which will constitute noise for electrical experiments. The spectrum of this noise is unknown.

The noise is expected to be spectrally different on the solar side as opposed to the anti-solar side of the moon.

3.4.3 Modes of Propagation in Solar Plasma

The mere presence of a plasma around the moon leads to the observation that antennas situated on or above the lunar surface will launch several modes of electromagnetic and acoustic waves. The dispersive behavior of electromagnetic waves in a stationary unbounded plasma may be described

in terms of a dielectric tensor (Brandstatter, 1963, p. 157)

$$K_e = \begin{bmatrix} 1 - \sum_r \frac{(\omega_{pr}/\omega)^2}{1 - (\omega_{gr}/\omega)^2} & i \sum_r (\omega_{pr}/\omega)^2 \cdot (\omega_{gr}/\omega) & 0 \\ -i \sum_r \frac{(\omega_{pr}/\omega)^2 \cdot (\omega_{gr}/\omega)}{1 - (\omega_{gr}/\omega)^2} & 1 - \sum_r \frac{(\omega_{pr}/\omega)^2}{1 - (\omega_{gr}/\omega)^2} & 0 \\ 0 & 0 & 1 - \sum_r (\omega_{pr}/\omega)^2 \end{bmatrix} \quad (1)$$

where $\omega_{pr}/\omega = \left[\frac{N_{0r}\, e^2_r}{\varepsilon_0\, M_r\, \omega^2}\right]^{1/2}$ is the ratio of the plasma (ω_{pr}) and applied (ω) frequencies for the r-th species in the plasma $\omega_{gr}/\omega = \frac{e_r B_0}{M_r \omega}$ is the ratio of the gyro-frequency to the applied frequency for the r-th species; M_r and e_r are the mass and charge of the r-th species, respectively; B_0 is the scalar magnetic field oriented in the z direction; N_{or} is the number density of the r-th species; and ε_0 is the dielectric permittivity of free space. For the interplanetary medium, we may consider protons and electrons as the only species present.

Equation (1) immediately informs us that the dielectric behavior is anisotropic, is a function of frequency, and exhibits resonances. At any frequency significantly above the electron plasma frequency, say at 0.7×10^5 Hz, the dielectric tensor reduces to a scalar with the free space value of unity.

If we now introduce the boundaries between the plasma and the moon's surface and between the plasma and the antenna, the problem becomes considerably more complicated except at frequencies above 0.7×10^5 Hz. Thus, we cannot simply relate the antenna pattern to the conductivity distribution within the moon at frequencie less than about 0.7×10^5 Hz on the solar side of the moon.

However, the problem is even more complicated, for description of both the electromagnetic and the acoustic modes requires the introduction

of a compressibility tensor as well as a dielectric tensor (Phillips, 1968). The importance of pressure gradients may be seen in Ampere's law (Phillips, 1968) for frequencies above the electron plasma frequency

$$\nabla \times \vec{H} = i\omega\epsilon_0 \left\{ \tilde{\tilde{K}}_e \vec{E} - (\xi_e / N_0 e)\, \tilde{\tilde{C}}_e\, \nabla p_e \right\} + \vec{J}_e \qquad (2)$$

where $$\xi = \frac{\omega_{pe}^2}{\omega^2 - \omega_{ge}^2}$$

ω_{pe} = electron plasma frequency
ω_{ge} = electron gyro-frequency
ω = source frequency, radians/sec.
$\tilde{\tilde{K}}_e$ = dielectric tensor
$\tilde{\tilde{C}}_e$ = compressibility tensor
∇P_e = gradient of perturbation plasma electron pressure
$\vec{J}_e$ = electric source term

Actually, Phillips notes:

"The type of pressure wave existing divides the frequency axis into three natural regions. Above the electron plasma frequency at $\sim 2.8 \times 10^4$ Hz, we assume, because of Landau damping, only an electron pressure wave exists. This pressure wave probably is damped out at approximately 1×10^2 Hz), the electron pressure wave is cut off or is at least appreciably below the ion wave in energy, and we consider that only the ion pressure wave may exist in the lower part of this region

"Below approximately the ion plasma frequency we consider a MHD region where the ions and electrons oscillate together as a single sound wave in the gas. Here, we consider Alfven waves and the hybrid magnetoacoustic waves."

Note that in the plasma "void" on the anti-solar side of the moon, the medium surrounding the antenna would look like free space for frequencies at least down to 10^3 Hz.

Phillips notes that for an orbiting antenna, the plasma will interfere with propagation at frequencies between the electron plasma frequency at 2.8×10^4 Hz, and the frequency where the plasma looks like free space,

say, 0.7×10^5 Hz. However, below 2.8×10^4 Hz and above, say, the electron gyro-frequency, there is effectively no electromagnetic propagation from an orbiting antenna.

It is therefore concluded that the plasma will not affect the proposed experiment, for which the lowest frequency is 10^5 Hz.

3.4.4 Plasma Sheath Around the Antenna

No attempt has been made in our studies to date to evaluate the effect of the antenna plasma sheath. However, it is reasoned that since the lowest frequency employed is 10^5 Hz, the antenna plasma sheath should not affect the proposed experiment significantly.

3.5 The Possible Lunar Ionosphere and Lunar Plasma Sheath

3.5.1 The Lunar Surface Electric Field

The particle bombardment of the lunar surface can lead to static and dynamic electric fields near the surface. However, this is but one mechanism for the generation of electric fields (Rycroft, 1965). There will be a static $\vec{v} \times B$ term arising in induction by the interplanetary field (Sonett, Colburn, and Currie, 1967), a dynamic induction term arising in transients in the interplanetary field (Sonett, Colburn, and Currie, 1967), a photon bombardment field, and possibly a cosmic ray bombardment term. All of these processes can lead to the production of a lunar atmosphere and to ionization of the atmosphere and lithosphere. According to Rycroft (1965), these processes compete and it is not clear (a) whether the moon retains a net negative or positive charge or (b) whether the assumed lunar ionosphere is positively or negatively charged relative to the lunar surface. Further, very little can yet be said of the transient behavior of these fields. Any charge accumulation on the lunar surface may not be experienced beyond a Debye length into the solar plasma and this is of order 10 meters (although an electron gyroradius of about 1 km may be a more appropriate number than a Debye length).

Petschek (1965) suggests static electric fields of order 0.1 to 100 volts per meter for the first 10 to 100 meters above the lunar surface.

3.5.2 Reflection from the Lunar Ionosphere

The condition for transmission of an rf sinusoidal pulse in an ionized gas is given approximately by:

$$f \geq 0.9 \times 10.3\sqrt{N_e} = f_p \text{ Hz} \qquad (3)$$

where N_e is the number of electrons per cm^3. When f is equal to f_p, the wave is reflected.

The time delay and transmission frequency thus map the electron-density profile in the same manner as topside or bottomside sounders on earth.

It is clear that the sounding can measure only an electron density that increases with distance from the spacecraft. The lowest proposed frequency is 10^5 Hz, so that a density of about 100 electrons per cm^3 is required for reflection; a factor of 10 increase in electron density above that of the free stream solar wind is thus required for lunar ionospheric reflection.

At present, theories regarding the electron density of the lunar ionosphere are based on quite arbitrary assumptions. The lunar ionosphere could consist of a single layer with a maximum density of the order of 100 electrons per cm^3 (Weil and Barasch model) derived from an atmosphere having a maximum density in the range of 10^6 to 10^{10} particles per cm^3. It would be expected to depend markedly on solar wind particle flux, solar ultraviolet flux, and the interplanetary magnetic field, as well as the properties of the lunar surface. The only quantitative estimate of the lunar ionospheric density is provided by the Stanford bistatic occultation experiment (Eshleman, 1967), and while it provides an estimate of a maximum density of 44 electrons per cm^3, it really only measures the vertical gradient of electron density and inserts this in the Weil and Barasch model to predict a maximum density estimate. It is not at all certain whether the maximum in electron density will occur above or below the spacecraft nominal altitude of 100 km. However, whether or not such a maximum does indeed occur <u>above</u> or <u>below</u> the spacecraft, the electron density profile to such a maximum can be measured, assuming $f_p > 10^5$ Hz. If the maximum lies between the

spacecraft and the lunar surface, this can possibly be determined by effects on the pulses whose frequencies barely permit penetration through the plasma, which are reflected by the lunar surface, and return through the plasma to the spacecraft.

On one extreme, there is no assurance that a lunar ionosphere exists. On the other extreme, a dense ionosphere could render difficult measurements of the electrical parameters of the lunar interior. Detection of an ionosphere, by means of the proposed experiment, would constitute a fundamental contribution to our knowledge of the moon and its environs.

3.5.3 Reflection from the Lunar Surface Plasma Sheath

Reflection from the postulated lunar plasma sheath must be considered in interpreting results from the lunar surface. Little experimental knowledge is currently available with which to guide estimates of the importance of a sheath in the frequency range of interest, although the ALSEP plasma experiment is expected to provide much help in this direction. The unknown static value and the dynamic range and frequency range of transient electric fields at lunar surface renders any evaluation dubious.

Burtis and Linlor (1970) provide the following evaluation of the problem:

> "A sunlit body in a hot plasma may be charged to a d.c. potential relative to the plasma by several competing processes. A tendency to develop a negative charge results from the generally higher thermal velocities of electrons compared to protons, giving a higher random electron current to the body. This is opposed by photoemission of electrons from the sunlit surface, and by secondary emission of electrons due to particle bombardment, as well as other processes. Between the body and the neutral plasma is a 'sheath' of unbalanced charge extending over approximately one Debye length.
>
> "For the case of the moon, most investigators have concluded that the photoelectron effect is dominant, and consequently that the sunlit lunar surface is positively charged. Table I gives several models. Heffner (1965) balanced the escaping photoelectron current with the solar wind thermal electron current on a global basis. His 'overestimate' model, based on a large value for the emitted

TABLE 1

PUBLISHED MODELS OF LUNAR PHOTOELECTRON SHEATH

MODEL	SURFACE POTENTIAL, volts	SURFACE E-FIELD, volts/cm	SURFACE DENSITY, el/cm^3	INTEGRATED DENSITY, el/cm^2
HEFFNER "OVERESTIMATE" (1965)	+32	1.6	2.4×10^5	8.8×10^5
HEFFNER "REALISTIC" (1965)	+18	0.16	2.4×10^3	8.8×10^4
GROBMAN AND BLANK (1969)	+0.6 TO +10.2	—	—	—

photoelectron current gives the largest values for surface potential (+32V), surface electric field, and surface electron density. The integrated density over a square cm column, which we note in this case is about 10^6 electrons per cm^2, is proportional to the surface electric field by Gauss' Law. Assuming a more realistic photoelectron flux, two orders of magnitude smaller, Heffner (1965) found somewhat lower values for the sheath parameters. Grobman and Blank (1969) used a more sophisticated photoelectron energy distribution and solved for local current balance. Depending on surface quantum yield and work function, they found potentials of from 0.6 to 10.2 volts at the subsolar point with lower potentials toward the limb. They did not solve for the surface field or number density.

"While the electron density may be quite large at the surface in such a sheath, it decreases rapidly with height. Figure (5) shows the density distribution for Heffner's over-estimate model; over half the electrons are within 2 cm of the surface. [Such a thin layer is not expected to produce a measurable reflection with the Lunar Electromagnetic Sounder.]

"It is well to keep in mind the limitations of this study. Collisions of electrons with the lunar surface have been neglected. These may be important at low frequencies where, if they absorb sufficient energy, they may decrease the reflection coefficient below the no-sheath value. Resonances have also been ignored. However, it appears from these calculations that radio sounding is not a suitable method for measuring a lunar surface sheath of the size expected. Conversely, the effect of the sheath on radiosounding of the subsurface is expected to be quite small." Detection of a sheath would be a significant contribution of the proposed experiment."

3.6 The Height of the Antenna Above the Lunar Surface

In a strictly analytic fashion, Dey, Morrison, and Ward (1970) have demonstrated that an electric dipole antenna at 100-km altitude appears as a plane wave source at the lunar surface at frequencies well above the plasma frequency.

The same situation is expected to pertain if the antenna is brought several tens of kilometers nearer the lunar surface. Thus, the only basic effect of changing the orbit height is expected to be a resulting change in the strength of the reflections from the lunar surface and subsurface, provided the pulse length is modified accordingly. If either a lunar ionosphere or a lunar plasma sheath exists, change of orbit might affect amplitudes and spectra of these reflections from those of the lunar interior. On the other hand, the lower the orbit, the higher the amplitude of the lunar reflections, and the greater the resolution of adjacent features on the lunar globe.

We may safely conclude, at this stage, that electromagnetic reflection from the lunar surface and subsurface is adequately described by plane wave formalism and that orbital height, while not critical, is best reduced as much as is feasible, since resolution is high in priority.

3.7 Scattering from the Rough Lunar Surface

Surface roughness, though defined arbitarily, is a function not only of the surface parameters of slope or height distributions, but also of the wavelength, polarization, and angle of incidence of the incident electromagnetic radiation. It is well-known that surface roughness can modify the returned signal much more than can the electrical properties of the half space (Beckmann and Spizzichino, 1963). This modification can reduce the ratio of the specular component of reflection to the diffuse component, which differs randomly in phase and in amplitude from the specular return.

The time delay of a reflection from an inclined surface face located at some lateral distance x from the sub-radar point of the Lunar Electromagnetic Sounder may be identical to the time delay of a reflection from a buried interface beneath the sub-radar point, if the following relation holds

$$t_o = \frac{\sqrt{x^2 + d_o^2}}{V_o} = \frac{d_o}{V_o} + \frac{d_1}{V_1} = t_1 \qquad (4)$$

where

x is the lateral position of the inclined reflector from the sub-radar point

d_o is the vertical distance from Lunar Electromagnetic Sounder to the lunar surface ($\sim$100 km)

d_1 is the depth beneath the sub-radar lunar surface to a buried reflector

V_o is the velocity of propagation of electromagnetic waves above the lunar surface

V_1 is the velocity of propagation of electromagnetic waves in the lunar interior above the buried reflector.

While Equation (4) can readily hold true for many possible configurations of the lunar surface and subsurface, it does not rule out recognition of sursurface layering in areas of rough lunar topography. Four factors facilitate recognition of off-vertical from vertical echoes, as follows:

1. The echoes received from interfaces off of the vertical plane normal to the velocity vector are Doppler-shifted because of the spacecraft orbital velocity. (Synethetic aperture analysis permits extraction of echoes which are zero Doppler-shifted.)

2. The dispersion (i.e., frequency dependence of phase and amplitude) of off-vertical inclined surface reflectors is expected to be different from the dispersion of on-vertical subsurface reflectors.

3. The polarization of off-vertical inclined surface reflectors is expected to be different from the polarization of on-vertical subsurface reflectors.

4. Given an optical description of the lunar surface, precise computation of the surface topographic scattering can be calculated using integral equation formulation for electromagnetic scattering (Parry, 1969; Hohmann, 1970).

Of course, off-vertical buried reflectors might be confused with on-vertical buried reflectors, provided the travel times of reflections are identical. Resource must then be made to synthetic aperture analysis plus different spectral, phase , and amplitude characteristics for

off-vertical and on-vertical reflections to facilitate distinction between the several sources of reflection. The virtue of a moving electromagnetic system for aid in this distinction becomes obvious. Perhaps, in this sense, the portrayal of ocean bottom depths, and sub-ocean bottom interfaces beneath an irregular ocean floor by means of omnidirectional sonic sounding is a suitable analogy for the current electromagnetic sounding application.

Airborne radar flown over glaciers in mountainous terrain in Greenland and Antactica has produced excellent profiles of both surface and sub-glacier topography and has permitted the identification of water, as opposed to rock, beneath the glacier. Depth of exploration in this terrain, which may be quite similar in electrical properties to the moon, has exceeded 14,800 feet (4.2 km) through ice. A newspaper account (Sullivan, 1969) of such sounding is included as Appendix I. Quoting Sullivan, "The radar beam, in the suitable frequency range from 20 to 100 megahertz, is very wide, and hence, additional echoes are obtained from surfaces not directly beneath the plane." "This generates some rounding of the inscribed profiles, if the terrain is rough, but the distortion can be removed. A computer method to this end is being devised here [Cambridge, England]. It has been found that the radar measurements are generally as accurate as those made with [sonic sounding]."

The principle differences between the terrestrial airborne and the lunar orbital electromagnetic soundings lies in the following characteristics:

Terrestrial airborne	Lunar orbital
2×10^7 Hz < f < 10^8 Hz	10^5 Hz < f < 2×10^7 Hz
altitude < 1 km (presumed)	altitude $\sim$100 km.

The reflections from surface topography, buried topography, and buried inhomogeneities will be most pronounced when the wavelength, at surface or in the subsurface, approaches the dimensions of the object under consideration. An upper frequency limit of 2×10^7 Hz for the proposed experiment assures that no object larger than about 15 meters in maximum dimension will produce a diffuse reflection. For an object of this dimension, the

spectrum of electromagnetic reflection near 10^7 Hz is expected to change dramatically with frequency and quite possibly to be characteristic of wavelength-sized scatterers as opposed to the spectrum of reflection from much larger objects of different electrical parameters. Polarization of the reflected electromagnetic waves is affected in a manner similar to the spectrum and can be diagnostic of objects of the size of a wavelength.

A surface and subsurface model of any degree of complexity presumably can be established and the plane wave reflection therefrom computed. A very simple model of topographic scattering is portrayed in Figure 6, (after Parry, 1969), where a two-dimensional ridge is described. Figure 7 illustrates the scattered magnetic field components. The model selected for these computations pertains to the earth so that conduction currents predominate over displacement currents. Extensions to this new theoretical achievement are visualized as follows:

1. plane wave reflection from two-dimensional surface, conduction and displacement currents both of importance, quasi-static solution (applicable below $\sim 10^5$ Hz)
2. plane wave reflection from two-dimensional surfaces, conduction and displacement currents both of importance; complete solution applicable at all frequencies
3. plane wave reflection from three-dimensional surfaces, conduction and displacement currents both of importance, complete solution applicable at all frequencies
4. same as 3) above but add subsurface interfaces
5. same as 4) above but add subsurface inhomogeneities.

Computations are currently in progress to solve item 1) above, and the extension to item 2) is straightforward. Formulation for the subsequent three steps appears to be within our grasp following about 36 man-months of effort.

Thus, it appears that we will be able to describe any hypothesized lunar structure and compute the reflection expected therefrom. By use of a number of reasonable models for each region of the lunar globe,

matches with observational data may be achieved. No unique interpretation is possible with this procedure nor should such be expected. However, on earth we have profitably used this same basic procedure in all geophysical investigations of the earth's interior.

Parallel to the theoretical computation of scattering from rough surfaces, one should expect to conduct scaled model experiments both to verify the theory and to extend it. Such model experiments are readily conceived and shall soon be in progress at U. C. Berkeley where a facility has been constructed for this purpose.

3.8 Scattering from Buried Interfaces Which may be Rough

In essence, this subject has been treated in the previous subsection. Philosophically, one does not have any substantial preconceived notion of the nature of buried topography, yet it is expected to affect the reflected electromagnetic energy. Quasi-specular reflection from inclined smooth surfaces falls approximately to 90% of its on-vertical value, assuming uniform field illumination for a lateral distance of 50 km from the sub-radar point on the basis of increased distance alone. This relatively small decrease with angle of incidence might suggest that off-vertical inclined interfaces can be major contributors to reflection whether they be at surface or sub-surface. Burns (1969a) notes that 50 percent of the quasi-specular reflection from astatic earth-based radar studies of the moon at 12-m wavelength occurs from within 4 degrees of the vertical. The problem is best described in terms of the convolution of the reflection coefficient with the quasi-specular scattering coefficient.

In any event, the sub-surface, off-vertical plane reflections are Doppler-shifted and may, accordingly, be distinguished from on-vertical plane reflections, provided adequate frequency discrimination is possible in the experiment.

Further, other sources of information such as photography plus active and passive seismic evidence may be expected to narrow the choice of subsurface models which will produce electromagnetic reflections approximating those observed. Once again, the analogies with seismic sub-bottom profiling and with radar sub-glacier profiling should be borne in mind.

We see no conclusive reason why the quality of the sub-glacier radar data obtained in Antactica with primitive equipment cannot be surpassed by a properly designed Lunar (orbital) Electromagnetic Sounder experiment.

3.9 Scattering from Buried Inhomogeneities

The integral equation approach to electromagnetic scattering permits computation of the reflection from buried inhomogeneities. Figure 7 depicts one component of the field scattered by a two-dimensional inhomogeneity of simple cross section. As noted earlier, these computations are being extended to suit lunar conditions. It would appear that any inhomogeneity, regardless of its complexity, can be modelled with this theoretical approach. Once again, scaled physical models will be used to check the theory and extend it to models for which computer time becomes excessive.

3.10 The Frequency Range of the Transmitted Field

The spectrum of the reflected electromagnetic fields can be diagnostic of the electrical parameter distribution in lunar subsurface as illustrated by Ward, Jiracek, and Linlor (1968, 1969) and by Jiracek and Ward (1970). Ionized pore water increases the amplitude of reflection from a buried interface and is expected to introduce a pronounced frequency dependence of dielectric permittivity. A frequency range of 10^4 Hz to about 10^8 Hz seems to be ideal for distinguishing a lunar model with ionized pore water, at depths within the first few kilometers of the surface, from a lunar model without pore water. The same range of frequencies is useful in deciphering concentric layering or mapping lateral changes in the electrical parameters. However, the ISIS A system, originally proposed as the basic hardware for the Apollo 19 Lunar Electromagnetic Sounder, is limited to the frequency range 10^5 Hz to 2×10^7 Hz. Reduction of the frequency range from 10^4 Hz to 10^8 Hz to the range 10^5 Hz to 2×10^7 Hz does allow slightly increased ambiguity in interpretation. Hence, reasonable effort should be made tc extend the range, particularly on the down-side. To insure accomplishment of this objective, a study must be made of the signal-to-noise ratios of antennas of various lengths: (Whether or not the ISIS A transmitter and receiver can be readily modified to permit downward extension of the frequency range is another question.)

The spectrum of reflections from discrete objects (diffuse reflections) and from surface or buried topography is expected to be of a different character than the spectrum of reflections arising in layered structures or in frequency-dependent electrical parameters. Subsequent integral equation evaluation of these latter spectral characteristics will be made.

Reflection from the moon in the frequency range 10^4 Hz to 10^8 Hz may be an oscillatory function of frequency if distinct uniform layering is present over distances of the order of the sampling area of a sounding. This latter area is difficult to define because the antenna pattern is broad and because specular, quasi-specular, and diffuse scattering are all involved. However, the rough estimate of a circular area of diameter equal to the height of the antenna above the lunar surface serves as a useful guide. True specular reflection arises only from the sub-radar point.

On the other hand, quasi-specular reflection from a distribution of inclined slopes extends out to substantial angles from the vertical, depending upon topographic relief. Thus, oscillatory behaviour of the reflection coefficient as a function of frequency may arise from very limited areas in those regions of the moon where surface and subsurface slopes are gentle and where diffuse scattering is minimal for the wavelength under consideration.

The lower the upper frequency limit, the less the scattering from rough surfaces and from small inhomogeneities. For this reason, the upper limit of 2×10^7 Hz for the ISIS A hardware would seem quite satisfactory, since objects smaller than about 15 meters (boulders and local topographic relief) will have little effect on the reflected energy. Objects larger than about 15 meters are geologically meaningful, so that measurement of reflection from them is important. The depolarized component is expected to decrease with decrease in frequency, as noted earlier, since objects small relative to a wavelength decrease in numbers with increase in size.

The decision to employ swept frequency (FM) or discrete frequency (FM) pulses centers around a desire to obtain precise calibration of the Electromagnetic Sounder System. Such calibration is more reliably made in the stepped frequency mode available in the ISIS A system; hence, that mode is selected. This decision then introduces consideration of the

number of frequency steps required to avoid aliasing of the reflection coefficient versus frequency curve, should an oscillatory reflection coefficient be encountered. Tentatively, fourteen frequencies have been identified as follows:

1.0×10^5 Hz	1.0×10^6 Hz	1.0×10^7 Hz
1.5×10^5	1.5×10^6	2.0×10^7
2.2×10^5	2.2×10^6	
3.4×10^5	3.4×10^6	
5.0×10^5	5.0×10^6	
7.0×10^5	7.0×10^6	

This selection of operating frequencies is to be re-examined subsequent to precise numerical computation of the antenna impedances, gains, bandwidths, and radiation patterns. Should any sharp resonances occur in the antenna characteristics, these may be avoided in the selection of operating frequencies.

Studies of the mechanical behaviour of the antennas attached to a dynamic Apollo spacecraft may force changes in lengths which in turn will affect the electrical characteristics and hence dictate the selection of fixed frequencies.

It has been suggested that an additional frequency, lying between 10^9 Hz and 10^{10} Hz, be utilized as a reference for radar description of lunar surface scattering characteristics. For frequencies this high, the diffuse component of reflection might well dominate over the specular reflection. Inclusion of an extra frequency in this band would not necessarily be an additional means of assessing the effects of lunar surface inclined slopes, but it would emphasize discrete scatterers of dimensions less than a wavelength.

To this writer, a more logical approach is one involving photographic description of the lunar surface to a resolution of the same dimension as the smallest diffuse scatterer for the wavelength transmitted by the Lunar Electromagnetic Sounder. Pursuing this further, a frequency of 2×10^7 Hz demands photographic resolution of order 15 meters, while a frequency of 2×10^9 Hz demands photographic resolution of order 0.15 m if surface scattering is to be deconvolved. Mere comparison of the backscattering at 2×10^7 Hz with that at 2×10^9 Hz serves no useful purpose wherever

unknown or unfavourable distributions of sizes of discrete scatterers or surface slopes is concerned. An unfavourable distribution in this sense is one which includes a greater number of scatterers, per unit area or volume of regolith, as size (i.e., as wavelength) decreases. The above comments pertain primarily to the expected component; the energy balance will shift toward the depolarized component as frequency increases according to radar observational evidence. This latter point will be discussed in more detail later. While one might commend the addition of a single higher frequency in some respects, a study is required to evaluate the scientific rationale and to determine the cost effectiveness of such.

3.11 The Polarization of the Transmitted Field

The transmitted field could exhibit any one of the following polarizations, depending upon the manner of excitation of one or more horizontal electric dipole antennas:

1. linearly polarized in horizontal plane, electric field parallel to spacecraft axis
2. linearly polarized in horizontal plane, electric field perpendicular to spacecraft axis
3. circularly polarized in horizontal plane, right-hand rotation or left-hand rotation.

The circularly polarized field would be generated by a pair of equidimensional orthogonal electric dipoles energized simultaneously but in phase quadrature. The advantage this configuration enjoys over linear polarization is that it permits measurement of the moon's impedance as a function of angle relative to the spacecraft axis, and this measures gross anisotropy. The aid in interpretation so provided is quite meaningful, since only by transmitting at all angles of incidence can all elements of the impedance tensor be measured. However, this polarization has been rejected for the proposed experiment because of the complexity involved in developing it for a spacecraft experiment designed to operate over a broad range of frequencies. This decision could be questioned.

Assuming then that circular polarization is not available, the only a priori reason to select one of the linear polarizations rather than the other, is to enhance synthetic aperture analysis. In this case, an electric dipole normal to the velocity vector is to be preferred to a dipole parallel to the velocity vector. However, later calculations may demonstrate that the spacecraft may have more effect on the antenna impedance, gain, and radiation pattern for a dipole oriented parallel to the spacecraft axis than for one oriented perpendicular to the spacecraft axis (or vice-versa). Of course, if the ISIS A configuration is retained, the first linear polarization will be used below 5×10^6 Hz, while the second linear polarization will be used above 5×10^6 Hz.

3.12 The Polarization of the Received Field

3.12.1 Radar Analysis

The expected component of radar echoes is defined as that component which would be received from a perfectly smooth surface. The depolarized component is orthogonal to the expected component and would not arise from a smooth surface. Earth-based astatic radar backscattering from the moon has demonstrated that most of the backscattered power is in the expected component, with the main contribution at meter wavelengths coming from a relatively small region centered on the sub-radar point. As the wavelength is shortened, the backscattered power from the bright spot near the sub-radar point decreases and the spot enlarges. At millimeter wavelengths the entire lunar surface has, very nearly, the uniform brightness seen at optical wavelengths. These observations indicate that the lunar surface is mainly smooth and undulating on a scale of meters; reflections from nearly flat surface elements oriented normally to the incident waves explain the central bright spot. The expected component from the bright spot is termed quasi-specular reflection.

That part of the reflection which is nearly uniform over the lunar disk, and which contributes most of the reflection at millimeter wavelengths, is termed diffuse reflection. Diffuse reflection may arise in surface or buried irregularities or inclined slopes whose dimensions are on the order of a wavelength or less. Evidently, at longer wavelengths the effects of

short scale inclined slopes average out, while the surface or buried irregularities are mostly smaller than a few meters in dimensions. Burns (1969 a,b) believes that most of the diffuse reflection arises in a volume distribution of various sized inhomogeneities in the regolith, the inhomogeneities following a third power cumulative size distribution per unit volume in order to satisfy a wavelength independence of the diffuse reflection between 23 cm and 12 meters wavelength. Whether the Burns' model is correct or will apply at the longer wavelengths proposed for the Lunar Electromagnetic Experiment is difficult to predict. If it does not, perhaps most of the depolarized power in the first echo would arise in inclined surface faces of dimensions less than a wavelength. If the latter assumption is made, then it would be possible to determine the distribution of surface slopes for comparison with photographic evidence. If the electromagnetic and photographic slope distributions do not agree, the conclusion might logically be drawn that the depolarized component arises in subsurface inhomogeneities. The importance of measuring both the expected and the depolarized components then becomes clear. In terms of the antenna system for the Lunar Electromagnetic Sounder, the expected component would be received on the same antenna as used for transmission, while the depolarized component would be received on an orthogonal antenna confined to a horizontal plane through the transmitting antenna.

3.12.2 Induction Analysis

Electromagnetic induction in a medium whose surface is rough or whose interior is either inhomogeneous or anisotropic or both, will yield a component of secondary or reflected electric field orthogonal to the primary or incident electric field. Knowledge of the orthogonal (depolarized) electric field component materially assists in interpretation of the shape and size of surface or buried inhomogeneities, or of the degree of anisotropy. Measurement of the secondary electric field components both parallel and perpendicular to the primary field permits less ambiguity in interpretation than does measurement of the parallel secondary field alone. A single inhomogeneity of geological importance will reflect, at long wavelengths, a component of inducing field normal to that transmitted. This situation really is identical to the depolarization, at radar wavelengths, from a distribution of small scatterers.

Thus, there is reason from this viewpoint to attempt to transmit on one antenna and receive on two orthogonal antennas as suggested earlier.

If the ISIS A antenna configuration is employed, then measurement of both polarizations is impossible. Further, the induction in the lunar interior will be different, within the low frequency band from 10^5 Hz to 5×10^6 Hz where the 240-foot antenna is employed, to that over the high frequency band from above 5×10^6 Hz to 2×10^7 Hz where the orthogonal 61.5-foot antenna is employed. Further, the crossover network used in ISIS A prohibits transmission on both the long and the short antennas at one overlap frequency. Hence, a jump in reflection coefficient might be observed at the crossover frequency of 5×10^6 Hz. This feature would seem to complicate interpretation slightly. The possible interpretational complication could be avoided with use of a different crossover network, with elimination of the crossover network, or by transmitting on one antenna and receiving on two orthogonal antennas. Such changes in experiment design require a detailed study.

3.13 The Location of the Receiving System Relative to the Transmitting System

An astatic experiment uses a single antenna for transmitting and receiving, while a bistatic experiment uses separate antennas which are spatially separated. If the spatial separation of the antennas can be varied, then the angle of incidence of the electromagnetic radiation may be used as a variable. Tyler (1968) has used this flexibility to good advantage to advance our knowledge of the distribution of electrical parameters in the moon.

For the Lunar Electromagnetic Sounder experiment, a bistatic configuration could be conveniently developed if both the Apollo spacecraft and a subsatellite of ISIS A dimensions were used for antenna locations. Insofar as a subsatellite of ISIS A dimensions is not included in the Apollo Orbital Science program, then a bistatic experiment is limited to orbital transmission and earth reception or vice-versa.

3.14 The Dispersion Spectra of the Electrical Properties of the Lunar Materials

The electrical conductivity and the dielectric permittivity of the lunar debris are known to be functions of frequency (Kopal, 1966, p. 369). In the debris the displacement currents dominate the conduction currents at radar frequencies and this condition is expected to pertain over the 10^5 Hz to 2×10^7 Hz band of the Lunar Electromagnetic Sounder experiment. Further, the dielectric permittivity of the debris is expected to be only a slowly varying function of frequency for frequencies above 10^4 Hz (Strangway, 1969). On the other hand, the conductivity is expected to increase linearly with frequency above 10^4 Hz (Fuller and Ward, 1970).

If ionized water or ice invades the pores of the lunar rocks at some depth, then the dielectric permittivity is expected to increase linearly with frequency above 10^4 Hz (Fuller and Ward, 1970).

If ionized water or ice invades the pores of the lunar rocks at some depth, then the dielectric permittivity is expected to be a more rapidly varying function of frequency while the conductivity is expected to be a more slowly varying function of frequency (Fuller and Ward, 1970).

Ward, Jiracek, and Linlor (1968, 1969) and Jiracek and Ward (1970) have demonstrated that such dispersion spectra of the electrical parameters materially affect the electromagnetic reflection coefficient for simple lunar models and in fact the resulting reflection coefficients may be diagnostic of the presence or absence of ionized water, for example.

3.15 The Doppler Shift of Off-Vertical Reflections

Synthetic aperture radar clearly demonstrates that it is possible to narrow, effectively, the antenna beamwidth by Fourier analysis of Doppler-shifted returns from a monofrequency transmission source (Brown and Porcello, 1969). Reflections arising from sources out of the vertical plane normal to the velocity vector are Doppler-shifted such that the effective antenna beamwidth is dictated by the inherent bandwidth limitations of Fourier analysis and by the spread of the Doppler shift across the antenna beamwidth.

To permit utilization of this technique for the Lunar Electromagnetic Sounder requires a receiver bandwidth sufficient to allow for the expected spectral spreading, a means for recording the received spectrum faithfully, a coherent detection scheme for comparing a field of received pulses and a computer program for separating the near-zero Doppler-shifted signals from the remainder. The required receiver bandwidth for this purpose is available in the ISIS A receiver.

The advantage in introducing this technique lies in its ability to reduce substantially the intensities of the off-vertical reflections (and so effect less ambiguity in interpretation) and to improve upon surface and subsurface topographic profiles of the type displayed in Appendix I. (The figure in Appendix I has been produced without synthetic aperture processing.)

The shorter the pulse of radiofrequency energy transmitted, the broader the spectrum of the transmitted field. On the other hand, the longer the pulse of radiofrequency energy, the less the time resolution of successive echoes from the top surface and a buried surface.

A study is required of the optimum pulse length and of the methods necessary to apply synthetic aperture analysis to the data to be received from the Lunar Electromagnetic Sounder.

4. Interpretation Procedures

4.1 Introduction

In the ideal electromagnetic experiment, one wishes to measure the reflected signal in the absence of any transmitted signal. Three alternative means for accomplishing this objective may be used:

1. In the first alternative, we transmit a pulse, of a given wave form, for a short time interval and measure the reflected signal after the pulse ends. The pulse length, the pulse repetition rate, and the pulse shape are selected to meet the needs of the experiment. Either astatic or bistatic configurations may be used.

2. In the second alternative, the receiver in a necessarily bistatic arrangement operates in a zero field unless a reflected echo is obtained. One simple means for accomplishing the condition of zero field is to reduce to zero (by geometrical orientation) the primary field received by the receiving antenna. A second means is that of monitoring only that phase component that is in quadrature with the primary field. A third means involves use of a small subsidiary transmitter to null out the field of the main transmitter at the receiver; provided the power output of the subsidiary transmitter is only a fraction of the power output of the main transmitter, reflections from it will be buried in noise.

3. A system relying solely upon measurement of the impedance of a single antenna, another alternative, is far from ideal insofar as one effectively measures the received signal in the presence of the maximum transmitted field intensity.

The first of the three alternatives has been selected for the Lunar Electromagnetic Sounder experiment because it is presumably much easier to implement than the second alternative, and presumably is superior in signal-to-noise ratio to the third alternative. This opinion could be questioned, but in an attempt to stay as close as possible to ISIS A hardware, we shall assume that it is correct.

For the experiment under consideration, the delay time t_o for return of a first echo from the lunar surface is given by

$$t_o = 2\frac{\sqrt{x^2 + d_o^2}}{V_o} \tag{5}$$

Assuming that most of the return is from the sub-radar point, we set x equal to zero and find that for an antenna altitude of 100 km, t_o = 667 μsec, from which we observe that the first return occurs 667 μsec from the leading edge of the transmitted pulse. Since time resolution of fractions of microseconds is readily achieved, we can expect that the reflected signal occurs well after the end of the transmitted pulse, unless the spacecraft effects a slow transient upon the assumed box-car function of transmitted rf energy. This assumption requires checking by procedures recommended subsequently.

For the moment, the received signal, consisting of the transmitted box-car truncated sinusoidal rf oscillation, modified by the transfer function of a region of the moon's interior, is recognized well after the cessation of the transmitted signal (Figure 8). The modulation of the received rf signal can be expected to rise quickly and decay slowly in amplitude and the received sinusoid may be shifted in phase relative to the transmitted box-car truncated sinusoid. The envelope of the pulse received from buried reflectors will be time-shifted relative to the envelope of the first received pulse, will be lower in amplitude, and will be of different shape. Measurement of the time delay, amplitude, and shape (pulse distortion) of the received pulse relative to the same characteristics of the transmitted pulse will contain the vital information concerning the transfer function of the lunar interior. Further, the phase of the rf oscillations will be shifted relative to those of the transmitted pulse. From these comments, it may be deduced that four measurements are desirable for the Lunar Electromagnetic Sounder Experiment:

1. measurement of time delay of the first and succeeding envelope echoes, relative to the time of the transmitted envelope (t_o, t_1, t_2, etc.)

2. measurement of the peak amplitude of the first and succeeding envelope echoes relative to the amplitude of the transmitted envelope (A_o/A_t, A_1/A_t, etc.)

3. measurement of the change of shape of the envelope of the first and succeeding echoes relative to the envelope of the transmitted signal (pulse distortion)

4. measurement of the phase shift of the rf oscillations as a function of time, of the reflected signal relative to the transmitted signal.

At this juncture, comment needs to be inserted relative to steady-state and non-steady-state operation of the Lunar Electromagnetic Sounder. The ISIS A equipment now in earth-orbit operates with pulse lengths of order 100 μsec. For all practical purposes, this pulse length permits treatment of the transmitted sinusoids as steady-state; the spectrum of the transmitted pulse is close to a delta function over the frequency range from 10^5 Hz to 2×10^7 Hz. In general, a wide receiver bandwidth is not required for steady-state, phase is readily measured for a long series of sinusoids, and the amplitude reflection coefficient is readily defined. On the other hand, if the pulse delay method of interpretation is to be invoked, pulse lengths as short as 0.2 μsec at 2×10^7 Hz (permitting four sinusoidal oscillations) are desirable with relaxation of pulse length (and still four sinusoids) to 40 μsec at 10^5 Hz. These latter conditions are strictly non-steady-state so that phase-delay of distinct reflecting horizons becomes synonymous with pulse-delay, while amplitude becomes synonymous with peak pulse amplitude from distinct reflecting horizons. The complex amplitude reflection coefficient, strictly speaking, is only defined in the steady-state, although it may be derived readily from single pulse characteristics. The following discussion, then, must be interpreted in light of the above comments.

4.2 Astatic Measurements

4.2.1 The Time Delay Method of Interpretation

Measurement of time delay of the first reflection of a continuous wave, being relatively unambiguous for earth ionospheric sounding, is the main interpretational feature of the ISIS A topside sounder experiment.

This measurement is of limited importance for the Lunar Electromagnetic Sounder, as subsequent discussion will reveal. The time delay of the reflection of a pulse from the lunar surface arises primarily in the time of two-way travel from the spacecraft to the lunar surface and back to the spacecraft. A further time delay becomes important to the lower Fourier components due to phase shift of the reflection coefficient of the first layer; this contribution is expected to be small and is dependent upon the shape of the transmitted pulse. The phase shift of the rf oscillations is obviously related to this latter incremental time delay and would appear to be a more sensitive means of recording the same information.

Reflections from interfaces beneath the lunar surface may be much more delayed in time. Measurement of the relative delay time between the first and subsequent echoes therefore becomes one method of determining the distribution of electrical parameters in the lunar subsurface. A broad bandwidth at the receiver is required to ensure that second and subsequent reflections can be recognized in the dispersion tail (if any) of the first reflection. The time delay method of interpretation and its limitation by receiver bandwidth are illustrated in Figures 9 and 10, respectively. A short transmitted pulse length is essential to time resolution of reflections from two interfaces closely spaced so that non-steady state conditions must prevail. Backscattering from off-vertical interfaces will spread the arrival time of the first echo so that shallow interfaces may be obscured, as the Antarctic ice sounding of Appendix I reveals. Synthetic aperture analysis can be expected to reduce this ambiguity considerably. Further, the separation of reflections arising in off-vertical inclined surfaces from those reflections arising in buried interfaces exhibiting the same time delay may be aided by study of dispersion and polarization, by non-model-dependent minimum-phase deconvolution, and by deconvolving the observed data with the transfer function of the surface reflectors. This latter step is achieved through metric camera photographic description of the lunar surface, by assignment of a reflection coefficient thereto, and by subsequent computation of the scattering from the lunar surface. It may be that the summation of all of these techniques will be inadequate to reduce the spread of the first echo to the point where regolith bottom echoes can be recognized. This situation could pertain in

regions of rough surface topography but is apt to disappear in regions of gentle surface topography. In any event, there will be some depth within the lunar interior at which the spread of surface echoes will not obscure a subsurface reflection. (For the Antarctic ice sheet, the surface echo is spread as much as 1000 feet, depending upon local topographic relief, with equipment not using spectral analysis, polarization analysis, synthetic aperture analysis, nor deconvolution of surface roughness scattering. Further, part of the surface "clutter" shown in the illustration of Appendix I is known to arise in a succession of near - surface interfaces.)

Of course, another more fundamental limitation on recognition of an echo from the regolith bottom is inherent in the length of the transmitted pulse. A pulse length of 0.2 μsec provides non-overlap of regolith top and bottom echoes provided the regolith is 20-m deep and is assigned a velocity of 2×10^8 meters per second. Complete time separation of regolith top and bottom echoes is not essential to recognition of both but is highly desirable for this time-delay mode of interpretation. A pulse as short as 0.2 μsec infers four transmitted oscillations at 2×10^7 Hz. A pulse length of 40 μsec at 10^5 Hz provides four oscillations and a resolution of 2 km, only, at a velocity of 2×10^8 meters per second. Reduction from four oscillations to one in each pulse may be desirable if time resolution is to be improved. On the other hand, as the number of rf oscillations in a pulse decreases, the spectrum broadens, which then requires study of its effect on receiver bandwidth and synthetic aperture analysis. It is possible to operate the ISIS A topside sounder transmitter with pulses sufficiently short to release one rf oscillation only, although this is a marked departure from the original design. Once again, the comment is pertinent that a systems study is required to determine the optimum pulse length and shape.

In the time-delay method of interpretation, a velocity is assigned to each unit of each model of a suite of possible models which will provide the required distribution of time delays. Ambiguity arises because, for example, first-echo to second-echo delay times can arise in a wide variety of ratios of layer thickness to velocity. Such ambiguity is reduced by using frequency as a variable.

Locking of the rf oscillation, or oscillations, to the square wave modulation is essential to this mode of interpretation.

4.2.2. The Amplitude Method of Interpretation

The amplitudes of the first and subsequent reflections is also related to the subsurface distribution of electrical parameters. Measurement of the absolute accuracy, of the reflection coefficient, of order 1 db, in a reflected signal which is in excess of 100 db down from the transmitted signal, is desirable for diagnostic recognition of various lunar models; this absolute accuracy may not be achievable. Absolute calibration of the antenna gain is required if this measurement is to be effected. Antenna theoretical, scaled model, and full scale analyses are necessary to calibrate the antennas as functions of frequency and to attempt to assess the accuracy of the calibrations. Mechanical distortion during experiment operation can affect the antenna pattern and calibration to an unknown extent. Hence, an analysis of antenna mechanical behaviour is required, and once this information is obtained, the effect of antenna deformation on the antenna pattern and calibration must be assessed. The choice of antenna length and materials may be governed by this electrical-mechanical iterative analysis. Ultimately, it could be necessary to obtain motion photography of the antenna during experiment operation.

A dry lunar interior is expected to lead to electric field intensity reflection coefficients in the range 0.4 to 0.5 at 10^5 Hz, while if ionized pore water or permafrost occurs within the depth of exploration, then the same reflection coefficients at 10^5 Hz are expected to rise to lie within the range 0.65 to 0.90 (Ward, Jiracek, and Linlor; 1968, 1969, and see Figure 10). The actual values of reflection coefficients within these ranges is determined by the electrical parameters and thicknesses of the regolith, the underlying assumedly dry bedrock, and the water or ice containing layers.

The amplitude of the reflection coefficient is a function of frequency and its change with frequency may be interpreted in terms of the subsurface distribution of electrical parameters. For lunar models consisting of dry materials overlying moist materials or permafrost, the reflection coefficient

decreases with increasing frequency. The reflection coefficient will become an oscillatory function of frequency if the area sampled by the experiment is approximately plane-layered, with layering reasonably consistent over this area. To allow for this contingency, which may well occur beneath the circular maria, a density of frequency samples is required which will assure that the oscillations of the reflection coefficient are not aliased. It is for this reason that 14 narrow-band frequencies over the range 10^5 Hz to 2×10^7 Hz were originally selected. However, if broad bandwidth signals, say of the order of 0.1 megahertz at 10^5 Hz ranging to 5 megahertz at 10^7 Hz are transmitted and received, then far fewer frequencies would be required. Provided adequate Fourier analysis of returned signals can be effected, then smoothing or aliasing of the reflection coefficient will not result. Again, a systems study is required to evaluate this degree of freedom in experiment design.

For the amplitude method of interpretation, the moon at any one location is treated as analogous to a black box whose transfer function is required. Monitoring the amplitude plus the phase of the reflection coefficient over a broad frequency range is a desirable means for obtaining this transfer function. Monitoring of amplitude alone over the frequency range 10^5 Hz to 2×10^7 Hz permits distinction between alternative models of the moon — as Ward, Jiracek, and Linlor (1968, 1969) have demonstrated.

The relative amplitude of reflection coefficient is expected to be a function of position in space over the lunar globe, both because of lateral changes in surface roughness and because of lateral changes in the electrical parameters or distribution of electrical parameters with depth. A relative system calibration of precision 1 db in a received signal in excess of 100 db down from the transmitted signal would permit monitoring a relative reflection coefficiency as a function of frequency and of position on the lunar globe. Once the effect of lunar surface roughness was removed or minimized by spectral analysis, depolarization analysis, synthetic aperture analysis, and surface scattering deconvolution, then qualitative maps of the electrical parameters may be produced to yield a qualitative geologic map of sorts. Correlation of this map with other evidence would lead to a further understanding of selenological processes. A relative calibration of the sounder system would also permit recognition of the rate

of change of reflection coefficient with frequency and, as Ward, Jirecek, and Linlor (1968, 1969) have indicated, this quantity can be diagnostic of the presence or absence of ionized water or ice in the pores of the lunar rocks. Typical expected changes in electric field intensity reflection coefficient with frequency are:

Lunar interior	10^5 Hz	10^6 Hz	Mean change
dry	0.40	0.38	0.02 per decade
with ionized pore water or ice	0.85	0.65	0.20 per decade

Whether or not slopes of these magnitudes can be differentiated depends upon the precision of the relative system calibration.

If more than one echo is received from the moon per transmitted pulse, then the amplitude and phase shift of the second pulse relative to the first will permit development of a suite of lunar models which will fit this observed transfer function. The wider the range of frequencies used, the less the ambiguity in interpretation. If relative phase shift of the rf oscillations is not measured and recourse is made to measurement of amplitude alone, ambiguity will increase on that account. This potential method of interpretation does require system linearity and, quite possibly, a large dynamic range.

Throughout the quantitative amplitude of reflection coefficient mode of interpretation, numerous models of the moon are established, based on intelligent estimates of the electrical parameters in the various units of the model. Ambiguity in interpretation results, because a suite of models will fit the observed data. The number of models in the suite can be reduced by using as many experiment variables as possible. These variables include frequency and polarization.

A long pulse length, approaching steady-state sinusoidal rf conditions, would appear to be ideal for this method of analysis. Again, the proposed systems analysis is to be emphasized.

4.2.3 The Pulse Distortion Method of Interpretation

The shape of the received pulse relative to the shape of the transmitted pulse will also yield information on the subsurface distribution of the

electrical parameters. This pulse shape might change more for second and subsequent echoes than for the first (surface) echo because of differential subsurface attenuation and dispersion plus differential subsurface reflection efficiency of the individual Fourier components of the transmitted pulse. The delay time of off-vertical surface reflections may effect substantial changes in pulse shape.

Measurement of the pulse shape requires a sufficiently broad receiver bandwidth that the spectra of the reflected pulses are not seriously degenerated by the receiver. A fast rise time for the transmitted pulse is desirable at each carrier frequency, so that the spectrum of the transmitted pulse is rich in frequency content. A short pulse duration also aids in establishing a rich frequency content.

To a certain extent, this interpretational mode is redundant if frequency is varied over the band 10^5 Hz to 2×10^7 Hz, insofar as amplitude as a function of frequency or of time may be computed therefrom. Yet the possibility of redundancy in interpretational modes is highly attractive if ambiguity in interpretation is to be reduced to a minimum.

Relative calibration of the Sounder System plus precise knowledge of the transmitted waveform are both required if the pulse distortion is to be measured relative to the transmitted pulse. This procedure may not be practical. On the other hand, if the shape of the first reflected pulse is used as a reference, then neither calibration nor knowledge of transmitted pulse shape is required.

Pulse distortion is expected to be a function of the center frequency of the pulse spectrum, of spatial position over the lunar globe, and quite possibly of received polarization. Models of hypothesized lunar interiors are constructed from best estimates of distributions of electrical parameters and of pulse distortions computed therefrom. The theoretical and observed distortions, as functions of frequency and received polarization, are compared to yield a suite of possible models. Ambiguity is present as usual. The mere evidence of change in pulse distortion from one region of the lunar globe to the other, once surface scattering has been deconvolved, will serve as a basis for development of geological concepts of the moon to depths of the order of 10 kilometers.

Metric camera description of the lunar surface is essential to successful interpretation via the pulse distortion method. Deconvolution of the effects of the rough lunar surface is thereby facilitated.

The optimum transmitted waveform and pulse length for measurement of pulse distortion has not been studied and should be the object of an early investigation.

The sensitivity of pulse distortion to the thickness and electrical parameters of various lunar layers has been studied in a preliminary manner by Phillips and Morrison (1969). Further analyses of this type are required.

The distortion of one pulse may be obscured by arrival of the next pulse; this problem is similar to the time delay of pulses from successive layers and places a limit on resolution of those layers.

Locking of the rf sinusoids to their ostensibly square-wave envelope is essential to this interpretational method.

4.2.4 The Phase Shift Method of Interpretation

There is a phase shift, of a continuous wave associated with reflection at a planar lunar surface, according to the formula

$$r = \frac{Z_a - Z_o}{Z_a + Z_o} \qquad (6)$$

where Z_a is the complex apparent impedance of an equivalent homogeneous half-space and Z_o is the impedance of free space. The phase of r can readily range from 45 degrees to zero degree over the frequency band 10^5 Hz to 2×10^7 Hz for expected lunar models (Ward, Jiracek, and Linlor, 1969). Measurement of this phase shift requires a transmitted-to-received-pulse coherent detection scheme not currently available in the ISIS A Sounder. Further, the rf sinusoids must be locked to their square-wave modulation envelope, or this type of phase study becomes impossible.

An error in measured lunar terrain clearance of 2 m, the noise level of the laser altimeter, results in a measurement of time delay of the first echo of approximately 0.013 μsec. This time delay represents a mean phase shift from a planar surface of 0.5 degree at 10^5 Hz and a mean phase shift of 5 degrees at 10^6 Hz from the same surface. Thus, only over the lower decade of the frequency range of the ISIS A equipment can mean phase be considered a measurable quantity. However, the mean phase of the reflection coefficient, particularly when coupled with the amplitude of the reflection coefficient, is diagnostic of planar layering and frequency dependence of the electrical parameters.

Measurement of the mean relative phase shift between the first and subsequent reflections for continuous wave operation can also be quite meaningful in the sense discussed previously for negative amplitude measurement.

Off-vertical reflections also result in phase shift; the reflections out of that vertical plane normal to the velocity vector may be removed by synthetic aperture analysis. The mean phase shift referred to above presumably is dominated by the on-vertical phase shift.

Interpretation proceeds as for the procedures for the amplitude interpretation mode.

The transmitted-to-received-pulse coherent detection scheme required for the phase-shift method of interpretation is to be distinguised from the pulse-to-pulse coherent detection scheme required for synthetic aperture analysis.

Variation of phase shift as a function of frequency and of position over the lunar globe may be extremely useful for geological mapping, even in a qualitative sense. A procedure of correlation of phase shift, or phase shift as a function of frequency, with other evidence provided by geological, geochemical, or other geophysical evidence is inferred in this respect.

Phase shift could be a function of received polarization, for a given transmitted polarization, and this fact can aid the interpretational process.

A long pulse length, approaching steady-state sinusoidal rf conditions, would appear to be ideal for this method of analysis. The proposed systems analysis would provide the trade-off evaluations between long pulse requirements of amplitude and phase methods of interpretation versus the short pulse requirements of the time delay and pulse distortion methods of interpretation.

4.2.5 Other Factors

4.2.5.1 Pulse Repetition Frequency

The pulse repetition frequency (PRF) is optimized towards maximum resolution. To construct a synthetic aperture for each frequency, the PRF must adequately sample the Doppler bandwidth across the antenna beam. This equires a sampling rate of at least the Nyquist criteria (two per cycle) for the Doppler frequency at the beam edge.

For spectral interpretation over a number of frequencies, the difference in spacecraft position at the start and end of a sweep should be no more than a fraction of expected ground resolution. For the lower

frequencies in the experiment, the backscatter function may limit the ability to use synthetic aperture techniques. In this case, the pulse-to-pulse PRF for a particular frequency must be high enough to avoid aliasing of expected lunar geologic anomalies responding to that frequency.

A study is necessary to define the optimum PRF for all frequencies.

4.2.5.2 Dynamic Range

The dynamic range of the ISIS A receiver is about 56 db (amplitude). This is on the order of optical recorder dynamic ranges. Both types of dynamic ranges can be improved with pulse compression schemes. About 40 db can be added to the dynamic range by cycling the transmitter at, say, 4, 40, and 400 watts peak power. The impact of lowering the PRF for any particular frequency and power level, however, must be assessed in terms of the discussion in Section 4.2.5.1 above. A dynamic range of 30 to 100 db is thought to be adequate and necessary for a wide variety of lunar responses.

4.3 Bistatic Measurements

We shall assume in this section that bistatic measurements are limited to either transmission on earth and reception in lunar orbit (up-link) or to transmission in lunar orbit and reception on earth (down-link). Until now, bistatic measurements have been down-link only, utilizing lunar satellite communications transmitters and large dish receivers on earth. These measurements, while cleverly designed by Stanford University personnel, have suffered from an imperfect knowledge of the direction of the linear electric field polarization (Tyler, 1969; Howard, 1970). A preference clearly exists for transmission of at least one circularly polarized electromagnetic wave of known dependency of rotation angle upon time. Lacking this ideal, one can accept a linear transmitted field, provided one receives two orthogonal polarizations whose orientation is known relative to the transmitted polarization. Such is suggested as a strong realizable subsidiary utilization of the Lunar Electromagnetic Sounder experiment.

An up-link bistatic experiment could take advantage of the flexibility of high power and large transmitting antennas on earth, while the down-link experiment must rely upon modest transmitting power and antenna size, but achieves advantage in terms of high receiver gain. The following remarks, however, are predicated on the belief that the Lunar (orbital) Electromagnetic Sounder experiment offers advantages over a strictly bistatic experiment which necessarily involves an earth-based antenna. The trade-offs of strictly bistatic (one earth-based antenna) versus combined astatic and bistatic are discussed subsequently. In any event, we can illustrate bistatic lunar sounding adequately by restricting attention to a lunar-orbiting linearly polarized transmitter and an earth-based dual-polarization receiver.

Any local inhomogeneity, or collection of inhomogeneities, will give rise to a component of the electric field normal to that transmitted. This phenomenon is referred to as "depolarization." The greater the departure of a lunar model from concentric layering, either in terms of inclined surface and subsurface faces, or in terms of a single large inhomogeneity, or in terms of a surface or volume distribution of discrete scatterers, the greater the depolarization. Depolarization will be a function of frequency and potentially will be a function of the angle of incidence of the transmitted electromagnetic wave. Any error in knowledge of the direction of linear polarization of a transmitted wave will be reflected in an incorrect ratio of <u>polarized</u> to <u>depolarized</u> returns from the lunar surface. For example, for the Lunar Electromagnetic Sounder, a pointing error of 1 degree of the transmitting antenna will give rise a 2 percent observed apparent depolarized return, even where none exists. This fact requires that strict knowledge of the orientation of the space-craft axis be known at all times. Further, it requires that the orien-tation of the electric dipole antenna, relative to this axis, be known precisely at all times. Mechanical and thermal flexure, static or dynamic, of the transmitting antenna may obviate this knowledge. Cross-coupling between nonorthogonal or deformed antennas also becomes important in this respect. A mechanically stable antenna is therefore a prerequisite to reliable bistatic measurements of lunar electrical parameters. Thus,

a study of antenna mechanical behavior under static and dynamic forcing functions pertinent to the Apollo Command and Service Module (CSM) is a necessary early study. The expected forcing functions include thermal heating, spacecraft yaw and roll, spacecraft ejecta, and energy flow couplings between these forcing functions. The final mechanical antenna design then requires study for its electrical characteristics of antenna gain, radiation pattern, and input impedance.

One of the main features of a bistatic experiment is the opportunity to measure the Brewster angle, which permits estimate of dielectric constant independent of all other variables (Tyler, 1968). Tyler's reflectivity graph of relative power versus angle of incidence is contained in Figure 12. Jiracek and Ward (1970) have demonstrated that Tyler's value of ~ 3.0 for the dielectric constant of the regolith, obtained at 1.3611×10^8 Hz, could pertain only to the top few centimeters of the regolith if a reasonable model of a gradational regolith was experimentally investigated. (Figures 13 and 14). Further, for a lunar model of sharply layered dielectric constant values, large changes in reflectivity may be introduced by very small changes in regolith thickness. To provide less ambiguous results in a bistatic experiment, therefore, it is desirable to utilize a spectrum of frequencies rather than the single frequency so far available. The broader the spectrum of available frequencies, the less the ambiguity in interpretation. In particular, use of frequencies much less than 1.3611×10^8 Hz is required to assist in reduction of ambiguity and to assure the greater depth of exploration necessary for penetration of the regolith and evaluation of lunar body properties.

The reflection coefficient, for an electromagnetic wave polarized in the plane of incidence (in this case parallel to the lunar vertical plane passing through the electric dipole antenna) exhibits a marked variation with angle of incidence, and in fact, ideally passes through zero at the Brewster angle. Measurement of reflection coefficient as a function of angle of incidence then permits recognition of the Brewster angle (θ_B) at which the dielectric constant of a homogeneous half-space is given

$$K = (\tan \theta_B)^2 \qquad (7)$$

The reflection coefficient perpendicular to the plane of incidence increases gradually with change from low to high angles of incidence, and at the Brewster angle is orders of magnitude greater than the reflection coefficient for parallel incidence. Several factors give rise to non-zero values of reflection coefficient, parallel incidence, at the Brewster angle. These are as follows:

1. finite conductivity of a homogeneous half-space
2. cross-coupling error between the lunar orbital transmitted polarization and the two earth-based orthogonal received polarizations
3. aliasing of the reflection coefficient where the reflection coefficient is an oscillatory function of frequency plane layered structures
4. surface roughness including both quasi-specular and diffuse reflection.

The use of frequencies lower than 1.3611×10^8 Hz is highly desirable to obtain values of dielectric constant pertinent to depths beneath the regolith. Further, items 1),3),and 4) may be evaluated if more than one frequency is used for a bistatic sounding. The top frequency of the ISIS A topside sounder is 2×10^7 Hz, a frequency which can be expected to traverse the earth's ionosphere without attenuation. Below about 10^7 Hz, however, transmission to earth will be seriously affected by earth's ionosphere. Thus, in essence, a single frequency bistatic experiment is possible with the proposed Lunar Electromagnetic Sounder experiment. The frequency indicated is about an order of magnitude lower than used so far in bistatic experiments, and hence, expected to penetrate deeper into the lunar interior than heretofore possible by bistatic experiments.

To improve interpretation, at least one frequency higher than 2×10^7 Hz would also be desirable as an objective of the bistatic aspect of the Lunar Electromagnetic Sounder experiment.

Reception of a frequency of 2×10^7 Hz on earth is a matter that requires a study of the flexibility of existing earth-based antenna systems and the costs of operation of antenna facilities. Such a study is recommended.

Bistatic experiments have been operated to date solely in the amplitude interpretation mode. Only relative calibration of the receiving antenna on earth is required for determination of the Brewster angle. Relative calibrations of earth-based large-dish antennas are usually known to sufficient precision for this purpose.

The reflection coefficient is a slowly varying function of the angle of incidence near the Brewster angle, and this fact leads to errors in the estimates of dielectric constant.

The apparent dielectric constant for a layered structure, averaged over the sampling area, is obtained by a bistatic experiment. This apparent dielectric constant is not simply related to any true dielectric constant at a single frequency (Jiracek and Ward, 1970). Use of frequency as a variable aids in this interpretational aspect. The reflection at various angles of incidence in a bistatic experiment necessarily introduces averaging of dielectric constant over a broader area than a lunar orbital astatic experiment; lateral resolution is thereby sacrificed.

Tyler (1968) reported only 2 watts of useful power transmitted by the Explorer XXXV spacecraft so that signal-to-noise ratio of the bistatic experiment upon which he reported was a significant factor. For the Lunar Electromagnetic Sounder experiment, 400 watts of peak power are available, so that signal-to-noise power ratio should be enhanced by greater than 25 db.

4.4 Lunar Spherical Lens Experiment

As noted earlier, Salisbury (1967) proposed that the diffraction of electromagnetic waves in the 10^4 to 10^8 Hz range by the moon will be such that the field of an earth-based transmitter will be focused behind the moon. A receiver on a spacecraft passing behind the moon, according to this theory, can measure the extent to which the moon acts as a

spherical lens. The distribution of the electrical parameters of the moon can be deduced from the information so obtained. This is the up-link version of the "spherical lens" experiment. A down-link version involving lunar orbital transmission and earth reception is also possible.

Salisbury (1967) gives the gain of the moon as a spherical lens antenna as

$$G(\lambda) = \frac{4\pi^2 T(2R - T)}{\lambda^2} \tag{8}$$

where λ is the wavelength, T is the thickness of the lunar "crust" which is assumed to be transparent to electromagnetic waves, and R is the lunar radius. According to Salisbury, a transparent layer only 10-m thick can produce a gain as high as 70 db at 4×10^7 Hz.

Salisbury also gives the focal length of a spherical lens by the approximate formula

$$f = \frac{R\sqrt{K_e}}{2(\sqrt{K_e} - 1)} \tag{9}$$

From this relation we observe that the focal length is equal to or less than the radius R of the moon when $K_e \geq 4$. Under these circumstances the focusing cannot be observed. Dry volcanic ash has a dielectric constant of about 2 at 4×10^7 Hz and this would lead to a focal length of 1.7 R. Thus, the focal point occurs at about 1200 km beyond the moon's surface, on the moon-earth line, for this value of dielectric constant. If, on the other hand, we assume a dielectric constant of 2.8 as suggested by radar reflectivity studies, then the focal point is only 400 km beyond the moon's far side. Evidently, the location of the focal point is critically dependent upon the dielectric constant. The dielectric constants of dry basalt at frequencies less than 4×10^7 Hz is in excess of 4, so that the focal point would be interior to the moon if these rocks preponderate at the lunar surface.

Further, if the thickness of the "crust" is excessive, then aberration

will occur (Salisbury, 1967).

The attenuation must be neglibible in the "crust" so then the condition tan $\delta << 1$ becomes a constraint on this material for this experiment. This constraint may not be satisfied for rocks and soils of the types expected in the lunar environment.

Transmissions from Explorer 35, monitored on earth by Stanford University personnel (down-link), were at a frequency of 1.3611×10^8 Hz. Tyler (1969) concludes that focusing of electromagnetic radiation from the Explorer 35 transmissions are not in evidence. Use of lower or higher frequencies might alter this conclusion. Salisbury did advocate use of five frequencies within the range 2×10^4 Hz to 4×10^7 Hz. The Lunar Electromagnetic Sounder overlaps this band substantially, although attenuation through the earth's ionosphere at frequencies less than 10^7 Hz is large. Both up-link and down-link versions of the experiment are possible once the Lunar Electromagnetic Sounder is placed in lunar orbit. Excessive depth of the transparent layer, as deduced from the diffraction pattern of the moon, would be an indication of low conductivity and hence of low temperatures deep within the moon. Obviously, the lower the frequency, the more information can be derived about the deep interior of the moon. For a moon consisting of many concentric layers, the diffraction pattern would be complex for those frequencies which penetrated any number of layers. An inhomogeneous moon might not produce an obvious diffraction pattern.

Because the down-link version of this experiment has been in progress for some time and because no useful results have been reported from it, it seems doubtful that results can be expected from either the up-link or down-link versions. However, recognition of the possibility of this measurement is pertinent to this report. No change in Lunar Electromagnetic Sounder hardware or in procedures for data analysis is required to test Salisbury's theory. It does, however, require use of suitable earth-based antennas for transmission and/or reception.

4.5 Ambiguity in Interpretation

4.5.1 Introduction

Interpretation of the data will proceed as in the case of terrestrial electromagnetic exploration in the broad sense. That is, alternative initial models of the lunar interior will be evident from a preliminary scan of the data, then iterative procedures will narrow the selection of models. Further refinement may be obtained through additional information from other sources such as surface sample analysis, photography, passive seismic data, gamma-ray spectrometry, magnetometry, gravity field mapping, etc. The lunar surface electromagnetic experiment will be particularly important in terms of provision of control information at a local spot on the lunar globe.

As described earlier, measurements should be made of the amplitude, phase delay, time delay, and distortion of the received pulse. Correction for the receiver system and/or data link transfer functions is essential to extraction of the complex reflection coefficient r(f), the time delay, and the pulse distortion, all of which are related. Although one may interpret, for example, the complex reflection coefficient directly, physical understanding is aided by analysis employing such steady-state quantities as the apparent conductivity, $\sigma_a(f)$, and the apparent dielectric permittivity, $\varepsilon_a(f)$, given by:

$$\sigma_a(f) = \frac{1}{Z_o} Im\left[\frac{1 - r(f)}{1 + r(f)}\right] \tag{10}$$

$$\varepsilon_a(f) = \frac{1}{2\pi f Z_o} Re\left[\frac{1 - r(f)}{1 + r(f)}\right] \tag{11}$$

where Z_o is the impedance of free space and has the numerical value of of 377 ohms. In Equations (10) and (11) it is assumed that the lunar material is magnetically nonpermeable, and that the region above the lunar surface exhibits the electrical characteristics of free space. These assumptions are not necessary, but are convenient for the present discussion. The plots of $\sigma_a(f)$ and $\varepsilon_a(f)$ may be used directly to determine

the distribution of electrical parameters with depth on the reasonable assumption that the depth of sounding is inversely proportional to frequency.

For the time delay and pulse distortion methods of interpretation, auxiliary functions such as $\sigma_a(f)$ and $\varepsilon_a(f)$ are not essential. The time delay method provides a vertical geologic section, of sorts, once the velocity distribution is known or estimated. Other auxiliary functions such as $\sigma_a(t)$ and $\varepsilon_a(t)$ have been introduced for time domain interpretations (Phillips and Morrison, 1969). The Fourier transform relationships between frequency and time domain quantities are well known.

As noted earlier, there is always some ambiguity in interpretation of data from geophysical experiments and the present experiment is no exception. In the first instance, even for an idealized uniformly layered moon, the thicknesses and the electrical parameters of the layers may not be uniquely determined by electromagnetic sounding.

4.5.2 Reduction of Ambiguity

To reduce ambiguity, we have noted the following desirable features of a Lunar (Orbital) Electromagnetic Experiment:

1. Measurement of reflections over a broad frequency range.
2. Synthetic aperture analysis of resulting data (removal of Doppler shift).
3. Three-dimensional (metric camera) photographic description of lunar surface and subsequent deconvolution of surface scattering.
4. Measurement of terrain clearance by laser altimetry.
5. Evaluation of surface scattering by use of a single higher frequency (e.g., 10^9 to 10^{10} Hz).
6. Measurement of both polarizations.
7. Secondary bistatic measurements additional to primary astatic measurements.
8. Redundancy of interpretational modes including time delay, amplitude, pulse distortion, and phase delay methods.

A study of the relative importance of these factors to reduction of ambiguity is required.

4.5.3 Ambiguity in Detection of Pore Water

If one should consider detection of pore water in the lunar rocks as a high priority objective of the proposed experiment, then a review of the ambiguities in interpretation of data for this purpose is mandatory. We have previously noted that two characteristics of the reflection coefficient r(f) are typical of many rocks with more than a fraction of one percent ionized water. First, moist or wet rocks exhibit higher values of reflection coefficient than dry rocks as Figure 11 illustrates. Second, the change of reflection coefficient with frequency is more pronounced for moist or wet rocks than for dry rocks. The degree to which anisotiopy, inhomogeneities, and surface roughness will invalidate this analysis has not been examined to date. A detailed investigation of this topic will be made. Considering the great geologic importance that would be attached to detection of water on the moon, substantial analytic effort on this topic is warranted. The presence of water soluble ions is necessary to occurrence of high values of reflection coefficients arising in the water content of rocks.

4.5.4 Ambiguity Introduced by the Frequency Dependence of the Electrical Parameters

A frequency dependent dielectric constant and/or a frequency dependent conductivity can produce effects on the reflection coefficient similar to those produced by layering. Measurement of both amplitude and phase of the reflection coefficient reduces this ambiguity. Addition of the time delay method of interpretation also reduces this form of ambiguity.

If conductivity is a marked function of frequency then dry rocks are to be expected (Fuller and Ward, 1970), in which case displacement currents are expected to predominate over conduction currents. This results in conductivity becoming relatively unimportant. On the other hand, if dielectric constant is a marked function of frequency, then pore moisture is to be expected and this should be evident in high values of reflection

coefficient at low frequencies.

No serious ambiguity is therefore expected from this source.

4.5.5 Resolution

Two steeply dipping inhomogeneities at a distance x apart, may be resolved by the Lunar Electromagnetic Sounder provided the ratio $\frac{x}{h}$ is sufficiently large (h is the altitude of the spacecraft). Definition of the maximum resolution for steeply dipping structures will be made in subsequent theoretical analyses. This resolution is expected to be better than for gravitational field measurements and about the same as for ideal static magnetic field measurements.

The term resolution also may be applied to determination of the closest approach of two horizontal beds before they appear to merge as one. Studies of this item will also be made.

4.5.6 Detectability

The thinnest steeply or flatly dipping bed which may be detected depends upon the number

$$\theta = |kt| \tag{12}$$

where k, the wave number, is defined by

$$k^2 = \mu\varepsilon\omega^2 + i\mu\sigma\omega \tag{13}$$

and where t is the thickness of the bed. The detectability of the bed also depends upon the dielectric permittivity ε_s, the magnetic permeability μ_s, and the conductivity σ_s of the rock units surrounding the bed under study. Clearly, the angular frequency ω also enters into the problem. No simple answer to this problem can be given but estimates will be made by subsequent theoretical analyses for various depths of steeply and flatly dipping beds.

In the time domain, detectability of a thin bed is dependent upon the time delay it effects and upon its electrical contrast with its neighbors.

5. Experiment Requirements

5.1 Orbit

An orbit altitude of 100 km ± 20 km is quite acceptable. The tolerance indicated is purely nominal and, in fact, an orbit as low as 20 km would have merit in terms of stronger signal reflections, higher resolution, and less oblique return.

A circular orbit is preferred over an elliptical orbit because the electromagnetic illumination of the lunar surface would be independent of position in orbit.

A high angle orbit is preferred because it offers the possibility of a large areal coverage of the lunar surface if the experiment duration encompasses several orbits. An equatorial orbit is, however, quite acceptable.

Post flight knowledge of orbital position is required only in the sense that the Lunar Electromagnetic Sounder data must be precisely referenced to features on the lunar surface. A bore-sighted camera can provide the required referencing information on the sunlit side of the moon, but extrapolation of this knowledge based upon precise orbital parameters is essential.

5.2 Spacecraft Attitude

The antennas should be confined to a horizontal plane tangential to the orbit within a pointing accuracy of about ± 15°. This relaxed pointing accuracy stems from the fact that the antenna radiation pattern is broad and field strength falls off only according to the cosine of angle from vertical. All that is required is knowledge of what part of the lunar surface the antenna is looking at and this information is provided by a bore-sighted camera to the required precision.

Orbital rate control of the spacecraft is, however, required in order to ensure that the pointing accuracy is within the ± 15° limits.

5.3 Time Line

A 3-hour minimum continuous experiment duration is required.

This minimum provides for one and one-half orbits to permit the following experiment sequence: start on the sunlit side near the terminator, coverage over the sunlit side, coverage over the terminator, coverage over the dark side, coverage over the terminator, repeat coverage over the sunlit side, repeat coverage over the terminator, experiment end on dark side. The precise flight path, relative to the lunar surface, may be recovered by this process.

5.4 Lighting Constraint

Refer to the time line section for a discussion of this requirement.

5.5 Surface Constraint

Data over a topographically flat region is preferred to data over a region of high topographic relief, solely to minimize the scattering from off-vertical reflectors and so simplify interpretation. However, some gain in knowledge of the moon's scattering properties would be obtained by flying over both high and low relief areas.

5.6 Altimetry

A laser altimeter is desirable for obtaining altimetry to a precision of 2 m. A radar altimeter of precision 30 m would suffice, however, if transmitted-pulse-to-received-pulse coherent detection is abandoned. Precise control on free space attenuation and echo time delay is afforded by such altimetry.

The laser altimeter measurement rate of 400 per orbit is satisfactory for our purposes.

5.7 Bore-sighted Metric Camera

The bore-sighted camera is required for locating, periodically, the center point of the field of view of the Lunar Electromagnetic Sounder on the lunar surface. The metric camera rate of measurement of once every 10 seconds is satisfactory for our purposes as is its resolution of order 30 m.

6. Recommendations for Further Analysis

6.1 Antenna Theoretical Electrical Characteristics

6.1.1 Purpose and Objectives

The antenna impedance, gain, bandwidth, and radiation pattern (including the effects of the spacecraft) of the several possible configurations, which can now be identified as potentially suitable for the Lunar Electromagnetic Sounder, must be calculated. These calculations will permit selection of the optimum antenna or ascertain the trade-offs between alternate configurations. Thus, we visualize the following specific objectives of theoretical analyses of antenna electrical characteristics.

1. Assess the input impedance, gain, bandwidth, and radiation pattern of the ISIS A antenna configuration, as deployed near the spacecraft, as a first step in determining its suitability for the experiment. The ISIS A configuration consists of one 240-foot centerfed electric dipole and one 61.5-foot centerfed electric dipole, with the long dipole oriented parallel to the spacecraft axis. The long antenna covers the range 10^5 Hz to 5×10^6 Hz while the short antenna covers the range 5×10^6 Hz to 2×10^7 Hz. Polarization is then switched midway through the frequency range.

2. Assess the input impedance, gain, bandwidth, and radiation pattern of a *modified* ISIS A antenna configuration, as deployed near the spacecraft, as a first step in determining its suitability for the experiment. The modified configuration consists of one 61.5-foot centerfed electric dipole antenna oriented parallel to the spacecraft and an identical antenna oriented perpendicular to the spacecraft axis. With this configuration, transmission on one antenna and reception on two antennas over the whole bandwidth from 10^5 Hz to 2×10^7 Hz becomes possible and permits measurement of both polarizations. Initially, transmission on the antenna parallel to the spacecraft axis is to be analysed, but transmission on the perpendicular antenna may be made later. This transmitting dipole orientation is preferred because it assures maximum symmetry with the

spacecraft with resultant minimizing of variability in antenna electrical characteristics should the antenna deflect relative to the spacecraft. Further, deflection of the parallel dipole is expected to be much less than deflection of the perpendicular dipole.

3. Assess the input impedance, gain, bandwidth, and radiation pattern of a pair of 61.5-foot antennas oriented parallel and perpendicular to the spacecraft axis, as in 2) above, but with transmission on the perpendicular antenna. This configuration permits monitoring of polarization and is preferred for synthetic aperture analysis, as noted earlier.

4. Assess the input impedance, gain, bandwidth, and radiation pattern of a single 61.5-foot antenna oriented parallel to the spacecraft axis and deployed adjacent thereto. Polarization measurement is not possible with this configuration, but a single polarization transmitted over the entire frequency range would be permitted and thus any possible discontinuity in reflection coefficient versus frequency as obtained with the ISIS A configuration would be avoided. Preference for this orientation is the same as in 2) above.

5. Assess the input impedance, gain, bandwidth, and radiation pattern of a single 61.5-foot antenna oriented perpendicular to the spacecraft axis and deployed near thereto. The possible discontinuity in reflection coefficient at the midpoint of the frequency range is again avoided, while a preferred orientation for synthetic aperture analysis is obtained.

6. Assess the possibility of using antennas shorter than 61.5 feet and possibly thicker than the one-half-inch diameter initially intended for the configurations of items 1) through 5). If broad bandwidth is employed in reception and short pulses employed in transmission, natural electrical resonances of antenna configurations 1) through 5) may render the antennas unsuitable. Shorter antennas may obviate this problem. On the other hand,

narrow band reception and long pulse transmission as employed on the ISIS A sounder are not affected by antenna resonances, provided the operating frequencies are selected so as to avoid them. The shorter antennas offer greater mechanical rigidity. This could be an important factor for safety, stability of antenna calibration, and ensuring an adequate decoupling for polarization measurements. In this latter vein, a 1-degree mechanical deflection permits an electrical cross-coupling of one part in 60, so that the cross-coupled signal is only 35 db (voltage) down at this deflection. This is about the minimum rejection of cross-coupled signals that can be tolerated for reliable polarization studies. Possibly degeneration of this rejection to 20 db down (inferring a deflection of 6 degrees) could be tolerated. This would be an extreme, since the depolarized component may be much smaller than the expected component.

For the bistatic aspect of the experiment, it is essential that the alignment of straight antennas, relative to the spacecraft axis, be known to an accuracy of 1 degree.

It is anticipated that the calculations of antenna electrical characteristics will depend upon the results of calculationsof the antenna mechanical characteristics, so that an interative interplay between the electrical and mechanical studies is essential if the best compromise antenna design is to be achieved.

7. The decay of the transient eddy currents induced in the skin of the spacecraft requires calculation to determine whether or not electric fields resulting from eddy currents will overlap in time and amplitude with the electric fields received from the lunar surface. If they do, degradation of the signal-to-noise ratio may result. This, in turn, might result in moving the antennas farther than the nominal 3 feet from the spacecraft.

8. The pulse waveform resulting from a short input pulse to any one of the alternate antenna configurations must be evaluated, because of its impact on interpretation schemes.

6.1.2 Description of Theoretical Antenna Electrical Characteristics Study

The following descriptions of the procedures to be used to meet objectives 1, 2, 4, 6, and 7 above is provided as a means of indicating the approaches to be used. Objectives 3, 5, and 8 are to be left for definition until after items 1, 2, 4, 6, and 7 have been completed.

Task 1: Basic RF Study

The Apollo CSM and associated dipole antennas will be computer-modeled using an integral equation formulation. The characteristics of the antennas including mutual interaction with the CSM will be analyzed. Two dipole lengths, three antenna structure configurations, and nineteen separate frequencies will be considered. Dipole lengths are 240 and 61.5 feet tip-to-tip. The calculations will be performed at the following frequencies:

1.0×10^5 Hz	1.0×10^6 Hz	1.0×10^7 Hz
1.5	1.5	2.0
2.2	2.2	
3.4	3.4	
5.0	5.0	
7.0	7.0	

In addition, five additional frequencies will be chosen as required to reduce interpolation error between calculated frequency points. The three structure configurations to be considered are as follows:

A. 240-foot dipole parallel to the CSM axis
   61.5-foot dipole perpendicular to the CSM axis
   The long dipole will be excited over the frequency range 1.0×10^5 to 3.4×10^6 Hz. The short dipole will be excited over the range 5.0×10^6 to 2.0×10^7 Hz.

B. Two 61.5-foot antennas, one parallel and one perpendicular to the CSM axis. All nineteen frequencies will be excited on the dipole parallel to the CSM axis.

C. One 61.5-foot dipole parallel to the CSM axis. Calculations will be performed at all nineteen frequencies.

For each of the configurations above and for the antenna diameter (1/2 inch) composition (silver-coated beryllium copper), thickness (0.002 inch) and construction (interlocked) nominally planned for use in the Lunar Electromagnetic Sounder experiment.

a. The radiation pattern will be calculated to a model accuracy of $\pm$5% (0.2 db).

b. The antenna input impedance and the radiation resistance will be calculated to a model accuracy of $\pm$5%.

c. The echo signal received by the CSM after reflection from the lunar surface will be calculated to a model accuracy of $\pm$10% (0.4 db). The CSM will be assumed to be at an altitude of 100 km. Both a perfectly reflecting lunar surface and a two-layer finite conducting model above a perfect conducting plane will be considered. The reflection coefficient for normal incidence will be derived for the latter model and used to determine the surface-scattered field amplitudes for the specific surface model considered. The resulting short-circuit current and open-circuit voltage received at the antenna terminals will be determined for an antenna excitation level of 100 volts.

In the above calculations, the five unspecified frequencies will be chosen to reduce interpolation error. An interpolation error not to exceed $\pm$5% will be sought.

Task 2: Transient Analysis

The transient response of the CSM to an incident rectangular pulse of 10 μsec duration will be studied. The currents induced on the surface of the CSM will be calculated using a narrow Gaussian impulse excitation (duration ~ 33 nanosec). The time-constants for the buildup and decay of the current pulse will be determined from convolution of

the impulse response of the CSM with the 10-μsec rectangular incident pulse. A plane-wave pulse incident on the CSM will be employed. Greater refinement to be introduced, such as specifically modeling the three antenna configurations of Task 1 which excite the pulse, will be considered at a later time.

Task 3: Bandwidth

The bandwidth of the antenna configuration of Case A, Task 1, will be determined. Calculations at five additional frequencies will be made as required to define the passband more clearly.

Task 4: Recommended Configuration

Recommend an antenna configuration suited to broadband reception at discrete frequencies over the range 10^5 Hz to 2×10^7 Hz; antenna lengths are variables. Transmission on one antenna and reception on two orthogonal antennas is preferred. The objective is to ascertain the antenna configuration that provides the best compromise between wide bandwidths and reasonable antenna lengths for the Lunar Electromagnetic Sounder experiment.

6.1.3 Antenna Studies for a Single Higher Frequency

If a single frequency in the range 10^9 Hz to 10^{10} Hz is to be added to the basic Lunar Electromagnetic Sounder experiment, then a separate antenna will be required for that purpose. Under that option, the single frequency antenna might be mounted on the side of the Service Module of the Apollo spacecraft. This deployment then places the main antennas in the beam of the high-frequency antenna, so that scattering from the main antennas may affect results obtained with the high-frequency antenna. Further study of this problem is required in a manner yet to be specified.

6.1.4 Purpose of Tasks

The purposes for the above studies are as follows:

1. Assess the input impedance, gain, bandwidth, and radiation pattern of the ISIS A antenna configuration as a first step in determining

their suitability for the experiment. (One 240-foot and one 61.5-foot center-fed electric dipole.)

2. Assess a modified ISIS A configuration for an initial step toward the study of transmission of one linear polarization and reception of two orthogonal linear polarizations. (Two orthogonal 61.5-foot antennas.)
3. Assess a single 61.5-foot antenna to determine its suitability for transmission and reception over the whole bandwidth, thereby reducing the ambiguity introduced through switching to an orthogonal antenna midway through the passband.
4. Assess the importance of the spacecraft on the input impedance, gain, bandwidth, radiation pattern, and transmitted pulse decay rate for all three antenna configurations suggested in items 1) through 3) above.
5. Determine whether or not a shorter antenna of thicker cross section, or a different configuration might be more suited to broadband reception at a number of discrete frequencies over the range 10^5 Hz to 2×10^7 Hz. Polarization measurements are to be stressed for this analysis.

6.1.5 Conclusion

The above analyses, once performed, will serve as a guide for the antenna mechanical analyses to be described subsequently. An iterative interplay between antenna electrical and mechanical analyses is to be effected until the best compromise antenna design is achieved.

If a single frequency in the range 10^9 Hz to 10^{10} Hz is to be added to the basic Lunar Electromagnetic Sounder experiment, a separate antenna will be required for that purpose. Under that option, the single-frequency antenna might be mounted on the side of the Service Module of the Apollo spacecraft. This deployment then places the main antennas in the beam of the high-frequency antenna, so that scattering from the main antennas may affect results obtained with the high-frequency antenna. Further study of this problem is required in a manner yet to be specified.

6.2 Antenna Theoretical Mechanical Characteristics

6.2.1 Purpose and Objectives

Torsional oscillations, curvature oscillations, torsional deflections, curvature deflections, plus couplings between these deformations all require evaluation for the several antenna configurations described under Section 6.1. Forcing functions for static and dynamic deflections include solar radiant heating and changes therein during an orbit, nominal spacecraft active attitude control, unintentional large thrust gas-jet firings, gas-jet impingement, coriolis force during antenna extension, and gravity-gradient torque.

Three main classes of studies have been recognized:

1. In the interest of astronaut safety, the contingency case of antenna mechanical failure must be considered. One assumes that an attitude control jet remains open due to system failure. It will take the astronaut as much as 5 seconds to overcome this failure and a large thrust may be applied during this interval. If this contingency case occurs, antenna mechanical failure may or may not be invoked. While a provision is to be made to jettison the whole antenna package, this experiment-destroying procedure may not be necessary. Then the objectives of this class of study may be described as follows.

   Given the acceleration and duration of the contingency case, what will be the deflections of each of the alternative antenna configurations, and will failure occur for one or all of them?

2. If because of gross antenna deformation or failure, or for any other reason, it is necessary to jettison, pyrotechnically, the deployed antenna system, one wishes to be assured that the antenna will not be fouled on the spacecraft and so endanger astronaut safety.

3. With the spacecraft proceeding under nominal attitude control and the experiment already initiated, what effects on the electrical characteristics of the antennas will be inserted

by static and dynamic antenna deflections? In particular, we are concerned with dynamic changes in antenna impedance, gain, bandwidth, and radiation pattern, with static but experiment degrading departure from expected antenna impedance, gain, bandwidth and radiation pattern, and with static and dynamic degradation of polarization measurements through electrical cross-coupling associated with nonorthogonality of fundamental antennas. The additional case of departure of the antenna axes from orientations parallel and perpendicular to the spacecraft axes is of fundamental importance to the bistatic aspects of the experiment.

To meet the above three classes of objectives, the antenna mechanical studies described below are necessary.

6.2.2 Technical Description of Antenna Mechanical Studies

6.2.2.1 Antenna Extension

A short study will be done on extension dynamics. Since the space vehicle is not spinning, the severe limitation on extension rate imposed by coriolis buckling is not present. Nevertheless, the CSM is rotating once per orbit (relative to an inertial frame) and a net angular impulse must be applied to the system during extension. This impulse will be calculated. Also, the maximum deflection during extension will be given as a function of extension rate.

6.2.2.2 Nominal Operation

6.2.2.2.1 Description

Of the many sources of forces and torques under normal operation, only three would appear to be significant. These are: gravity-gradient/centrifugal, thermoelastic, and attitude control system interactions.

There are torques on the CSM and antennas, due to the fact that the antennas exist in either an inverse-square gravity field or in a centrifugal field. These two fields result in what is commonly called

the gravity-gradient torque. If the orbit is elliptical, there is no equilibrium position for the space vehicle, and it will experience a periodic torque proportional to the orbital eccentricity.

The thermoelastic torques and forces may be treated in three classes. In increasing order of analytic difficulty and in decreasing order of likelihood of occurrence, these are:

1. There will be a steady-state solar heating effect when the antennas are exposed to the sun. This will result in a constant curvature of the antennas, which will be superimposed upon any curvature resulting from manufacturing tolerance.
2. A transient version of this same phenomenon occurs when the spacecraft passes from shadow into sunlight.
3. A subtle effect known as"thermal flutter" arises in thermal-mechanical couplings. This phenomenon was investigated in a preliminary study carried out at NASA/GSFC. The results of that study clearly demonstrated the need for interlock of the edges of the pre-stressed "carpenter's rule" antenna material as it is unfurled from the spool on which it is stored.

An important interaction with the attitude control system is the effect of moments transmitted to the antennas from the spacecraft during the course of normal attitude control. In particular, the attitude control pulses may contain a large fraction of their frequency spectrum in the neighbourhood of the mechanical resonant frequencies of the antennas. A careful study is required to ensure that unacceptably large deflections do not result.

6.2.2.3 Attitude Control Contingency Case

The attitude control contingency envisages an attitude control jet remaining inadvertently open for a period of time before corrective measures can be taken by the astronaut. During this period, the spacecraft may undergo significant pitch, roll, or yaw. Limiting axis maneuvers are usually accepted as follows.

1. Roll-axis manuever

Acceleration of $4.5°/sec^2$ for 5 seconds, followed by a deceleration of $4.5°/sec^2$ for 5 seconds.

2. Pitch-axis maneuver

Acceleration of $2°/sec^2$ for 5 seconds followed by a deceleration of $4.5°/sec^2$ for 2.2 seconds.

3. Yaw axis maneuver

Same as the pitch axis maneuver.

If a pitch or roll error is introduced, the large inertia of the antennas, combined with their great flexibility, may lead to unacceptably large deflections. Just how large the deflections may become can only be obtained by computation. In addition, a large bending moment is impressed on the support boom.

If a yaw error is introduced, these remarks are still valid and, in addition, a large torsional moment is placed on the support boom.

6.2.2.4 Effect of Gas Jet Plume on Antennas

When the gas jets fire, the plume may be directed so as to impinge on an antenna. From information on the plume pressure, the resulting antenna stresses and deformations may be calculated.

6.2.2.5 Actuator Boom Dynamics

The dynamics of the total system, including both the actuator boom (boom for extending antenna module out a nominal 3 feet from the spacecraft skin) and the dipoles must be considered, because the motions of the boom affect the dipoles and vice-versa.

6.2.2.6 Other

Various means for providing improved thermal and mechanical behavior are available. The calculations described above would be on locked, silvered, beryllium copper, extensible carpenter's rule antennas of diameter 0.5 inch and material thickness 0.002 inch. It is known that perforated beryllium copper cylinders, blackened on the inside, exhibit much better thermoelastic behaviour. However, this improvement is achieved at the expense of mechanical strength in bending. Clearly then, diameter might be introduced as a variable.

Thermal flutter may be damped by use of small weights on the ends of the antennas. These and other factors could be studied if necessary.

6.3 Total Systems Analysis

6.3.1 Design Freedoms

Systems analyses are required to optimize the design of the Electromagnetic Sounder System. The design freedoms for an ideal experiment include:

1. pulse length as a function of frequency
2. pulse shape as a function of frequency
3. pulse repetition frequency
4. frequency range
5. number and placement of frequencies
6. addition of a single frequency between 10^9 Hz and 10^{10} Hz
7. bandwidth of receiver as a function of frequency
8. one or two polarizations
9. transmitted power and power steps
10. sequencing of powers and frequencies
11. transmitted-pulse-to-received-pulse coherent detection or not
12. antenna lengths, diameters, and configurations
13. modes of interpretation to be facilitated
14. recording medium
15. dynamic range of total system
16. data sampling rate
17. distance of the antennas from the skin of the spacecraft.

The degree to which a modified ISIS A system would permit freedom in design is currently under study. It is desired to adapt the ISIS A system designed for terrestrial ionospheric sounding to an optimum system for lunar solid body sounding within the monetary and time constraints. Once this has been achieved and the design frozen, then the precise

transfer function of the whole system is required so that the fidelity of the measured transfer function of the moon is known.

Significant departure from the ISIS A instrumentation is necessary for the ideal experiment. Increased receiver bandwidth, shorter pulses, faster transmitter rise time, coherent detection, and facility for recording both polarizations are desirable improvements over current ISIS A instrumentation.

6.3.2 The Effect of the System on Experiment Performance

Total systems analysis, with regard to the effect of the system on experiment performance, is to be based on a study of the following factors:

1. the type of reflection to be expected from each of a variety of lunar models for each of the four modes of interpretation
2. the spectrum, polarization, and Doppler shift of reflections from the lunar surface and buried rough interfaces
3. the resolution of adjacent thin layers or of adjacent inhomogeneities
4. the detectability of expected lunar inhomogeneities as a function of size of the inhomogeneity and as a function of frequency
5. the measured dispersion spectra of conductivity and dielectric permittivity of returned lunar samples as functions of added water content.

Degradation of the diagnostic characteristics of reflections, based on the foregoing factors, requires careful analysis, especially as each compromise is made relative to the ideal experiment. Thus, a rationale is required for establishing a priority rating of:

1. fast pulse rise time
2. short pulse length
3. wide receiver bandwidth
4. coherent detection
5. polarization information

6. bistatic measurements

7. extended frequency range to 10^4 Hz

8. addition of a single higher frequency.

6.3.3 Discussion of Design Freedoms

6.3.3.1 Pulse Length as a Function of Frequency

Summarizing from earlier discussions, we find the following requirements on pulse length:

1. 100 μsec at 10^5 Hz to 1 μsec at 10^7 Hz is reasonable for steady-state phase and amplitude measurement of 10 sinusoids

2. 10 μsec at 10^5 Hz to 0.1 μsec at 10^7 Hz is reasonable for the pulse delay measurement of a single sinusoid

3. 40 μsec at 10^5 Hz to 0.4 μsec at 10^7 Hz may be a reasonable compromise to permit steady-state phase and amplitude measurement plus pulse delay measurement

4. The optimum pulse length for the pulse distortion method of interpretation is unknown.

5. A pulse length of 0.1 μsec or shorter is required if the depth of the regolith is to be retrieved from the higher frequencies.

6.3.3.2 Pulse Shape as a Function of Frequency and Decay

Fast rise and decay times of the transmitted pulse are preferred if the pulse distortion method is to be used or if pulses of short duration are to be used, and also if maximum accuracy in measurement of pulse time delay is to be assured. Fast rise and decay times of the transmitted pulse are useful, however, only if a sufficiently broad receiver bandwidth is available at each frequency. These observations lead to the conclusion that a study is required of the following:

1. spectra of rf pulses of various frequencies truncated by realizable transmitter rise and decay times

2. spectra of the same pulses after reflection from each of a variety of lunar models

3. shapes, phase shifts, and amplitudes of the same pulses after reflection from each of a variety of lunar models

4. the rise and decay times to be expected from the ISIS A transmitter and from alternative transmitters

5. the bandwidths to be expected from a modified ISIS A receiver and from alternative receivers

6. the accuracy of delay time measurement, for each of a variety of lunar models, assuming various signal-to-noise ratios.

6.3.3.3 Pulse Repetition Frequency

The velocity of the spacecraft is about 1.65 km/sec when in lunar orbit. If all frequencies and three power levels are sampled once per second, one sounding will occur every 1.6 km. Considering the broad antenna pattern, this sample density appears to be adequate for resolution and delineation. It might be relaxed to once every two seconds if this were the only consideration. However, if synthetic aperture analysis is to be used, with no aliasing of the highest Doppler frequency, pulse repetition frequencies of 440 Hz and 2.2 Hz are required at transmitted frequencies of 2×10^7 Hz and 10^5 Hz, respectively.

6.3.3.4 Frequency Range

As noted by Ward, Jiracek, and Linlor (1968, 1969), extension of the lower frequency limit from 10^5 Hz to 10^4 Hz is desirable if wet and dry lunar models are to be differentiated. Greater depth of exploration and a reduction of surface scattering also result from this possible change. Two additional factors also bear upon this decision. First, coherent detection of the received pulse relative to the transmitted pulse is only accurate over the lower decade of the nominal ISIS A frequency range; by extending the lower limit of this range, twice as many decades are amenable to coherent detection. Second, solution of the surface scattering problem is expected to be much more difficult at frequencies in excess of 10^6 Hz than at lower frequencies. Computer storage and time consumption are also expected to be larger above 10^6 Hz than below; this factor may limit the flexibility of the models which can

be computer simulated. On the other hand, scaled model studies of scattering problems would still be available and useful at the higher frequencies.

Whether or not the antenna gain can be made adequate at 10^4 Hz has not yet been resolved, but a preliminary figure for several antenna configurations will be available once the studies of 6.1 are completed. These studies will need to be extended to cover the decade from 10^4 Hz to 10^5 Hz once the effect of frequency range on transmitter and receiver characteristics has been determined.

6.3.3.5 Number and Placement of Frequencies

Factors governing the number of frequencies to be utilized include receiver bandwidth at each frequency and a desire to avoid aliasing of an oscillatory reflection coefficient. Clearly, a decision on receiver bandwidth should be made prior to selecting the number and placement of the operating frequencies.

6.3.3.6 Addition of a Frequency Between 10^9 Hz and 10^{10} Hz

Because the antenna configuration to be used for the main frequency range is unsuited to use between 10^9 Hz and 10^{10} Hz, a separate antenna system for a single higher frequency in this latter range is a necessity. No study of the problem has yet been made, but it would appear possible that a completely separate transmitting and receiving system would also be required. The decision to add this feature presumably would center on cost effectiveness.

6.3.3.7 Bandwidth of Receiver as a Function of Frequency

The spectrum of the signal reflected $O(\omega)$ is governed by the spectrum of the transmitted pulse $T(\omega)$ as modified by the spectra of the scattering and reflection coefficients $S(\omega)$ and $R(\omega)$, respectively .

$$O(\omega) = T(\omega) \cdot R(\omega) \cdot S(\omega)$$

The receiver bandwidth must then be sufficiently broad to retain most of the information in $O(\omega)$. Actually, the spectrum of the pulse transmitted is related to the spectrum of the output of the transmitter power amplifier $P(\omega)$ by the relation

$$T(\omega) = P(\omega) \cdot A(\omega)$$

where $A(\omega)$ is the transfer function of the antenna. This same transfer function, for a linear antenna system, also enters into the signal received at the input terminals of the receiver $M(\omega)$.

$$M(\omega) = O(\omega) \cdot A(\omega)$$

It is required that $M(\omega)$ not be seriously degenerated by the receiver, so that computation of the function $M(\omega)$, for a variety of lunar models, is necessary before the receiver bandwidth as a function of frequency is established.

Since the transmitted pulse decreases in length as frequency increases, receiver bandwidth must increase with increase in frequency. Precise bandwidths are dependent upon the total systems study.

6.3.3.8 Polarization

To record both polarizations, a two-receiver system capable of measuring relative phase and absolute amplitude of two orthogonal electric field components is required. The degree to which the desired phase and amplitude accurancies of 1 degree and 1 db can be met is to be evaluated. Monetary and time constraints could rule out this design freedom.

Decoupling of antennas, an object of early studies on antenna electrical and mechanical characteristics, could rule out measurement of polarization.

6.3.3.9 Transmitted Power and Power Steps

The nominal 400-watt peak rf power output of the ISIS A equipment is satisfactory for the experiment. A sequential stepping down in 20 db power steps to 40 watts and 4 watts is highly desirable as a means of acquiring 40 db of additional dynamic range. Power-stepping influences transmitter sequencing and must, therefore, be studied in that relation.

Because the ISIS A obtains good signals from reflectors 3500 km beneath it in earth orbit, it is anticipated that the 400-watt operating level will provide a very substantial margin of safety for strong reflections from the lunar surface. It may, however, only just be an adequate power level to assure good signal-to-noise ratio from deeply buried interfaces. The decreased power levels permit placing the surface and shallow reflector signals within the dynamic range of the receiver and recorder.

6.3.3.10 Sequencing of Powers and Frequencies

Whether or not the ISIS A, or an alternative, transmitter can be sequenced as rapidly as desired is an object for study. If the desired sequencing rate is too high, then a reduction of the number of power steps, of the upper operating frequency limit (2×10^7 Hz), or of the number of frequency steps, must be made.

Possible sequencing rates are as follows:

Operating Frequency	Number of Frequencies	Number of Power Steps	Repetition Frequency	Sequencing Rate
2×10^7 Hz	14	3	440	18480
2×10^7 Hz	5	3	440	3520
10^5 Hz	5	3	2.2	17.6

6.3.3.11 Coherent Detection (T Pulse to R Pulse)

This feature would only be available below 10^6 Hz because of uncertainty of phase error associated with errors in laser altimetry.

Prior to considering it instrumentally, a study of its usefulness, in reduction of ambiguity in interpretation needs to be accomplished via computer modeling.

6.3.3.12 Antenna Lengths, Diameters, and Configurations

These factors will be studied under antenna electrical and mechanical analysis of 6,1 and 6,2 above. The impact of the selection of the optimum antenna configuration on the total system needs evaluation.

6.3.3.13 Modes of Interpretation to be Facilitated

A variety of lunar models, upon which plane electromagnetic waves are incident, is to be studied in terms of diagnostic information which may be deduced about them from pulse delay, pulse distortion, amplitude, and phase delay modes of interpretation. Early completion of this study is essential to several other design considerations. A priority rating of each interpretational mode can be expected to result from the study, so that one or more modes may be deleted on an objective basis if this proves necessary.

6.3.3.14 Recording Medium

Both telemetry-to-earth and photographic recording in the Scientific Instrument Module of the spacecraft have been considered as possible data recording methods. Telemetry is expected to constrain the experiment because of a data bit rate (or passband) lower than required. Photography constrains the experiment because of the requirement of EVA to recover the film cassette. A redundant system in which both photography and a limited telemetry scheme are employed has also been suggested. Real time monitoring of the experiment is possible with this latter scheme and is a highly desirable feature for any lunar orbital experiment.

Definitive information is required on the relative merits of photography, telemetry, and combined photography-telemetry data-recording processes.

6.3.3.15 Dynamic Range of Total System

The dynamic range requirement is unknown because of the unknowns in the lunar interior. The free path loss from antenna to lunar surface and return is in excess of 100 db. Loss on reflection at the first interface is only expected to be an additional few db. Loss

associated with attenuation in the lunar materials must be calculated assuming a wide variety of lunar materials and layerings. Studies of this nature, coupled with a study of anticipated range of noise levels, will provide information on the required dynamic range. The manner of achieving this dynamic range in the total system will also be studied.

6.3.3.16 Data Sampling Rate

The data sampling rate is dependent upon the recording medium used, the pulse repetition frequency, the power stepping, the number of frequencies used, the measured pulse waveform, and the mode or modes of interpretation to be used. Definition of sampling rate will follow from definition of these other parameters. If telemetry is used, some form of data compression may be necessary.

6.3.3.17 The Distance of the Antennas from the Skin of the Spacecraft

Antenna mechanical and electrical characteristics are dependent upon the distance the antennas are located from the skin of the spacecraft (the boom length). A nominal range of boom lengths of three feet to ten feet has been suggested by North American Rockwell but no decision on boom length has yet been made. This decision must be made at the earliest possible date since it determines the final antenna electrical and mechanical calculations. While awaiting this decision, the worst case of a 3 foot boomlength has been chosen for the electrical calculations and several lengths within the 3 foot to 10 foot range have been chosen for the mechanical calculations. These latter calculations could dictate the required boom length.

6.3.4 Synthetic Aperture Analysis

A study of the detailed requirements for, and gains to be obtained from, synthetic aperture analysis is mandatory. In particular, it is necessary to evaluate the percent of illuminated lunar surface which does not reflect within the zero doppler shift window, to establish an outline of procedures to be used in synthetic aperture analysis, to determine whether or not it should be applied over the whole frequency range, to determine whether or not its demands on data rates are feasible, and to assess its cost and time impact on the experiment.

6.3.5 Control Model Studies

Substantial effort is needed to develop a catalogue of control models for use in data interpretation and selection of segments of the lunar surface to be studied. In a manner analogous to interpretation of airborne geophysical data on earth, local anomalies of reflection coefficient will be interpreted quantitatively to reveal the range of subsurface models which is compatible with the observed data.

It is then necessary to identify the types of relections to be expected, and the means for recognizing features of these reflections which are diagnostic of quasi-specular lunar surface scatterers, quasi-specular buried scatterers, volume distributions of diffuse scatterers, individual large scale subsurface inhomogeneities, lunar subsurface layers, the lunar ionosphere, and the lunar plasma sheath. Field variables to be studied in a computer modeling program in development of control models include spectral response, polarization, spatial gradients, doppler shifts, and angle of incidence. The effects of these variables on each of the four modes of interpretation are to be investigated so that a priority rating of interpretational modes may be established.

Input for this study is to come from stereographic photography, frequent update of lunar interior and exterior knowledge, plus laboratory measurements of the electrical parameters of returned lunar rocks.

Where computer modeling becomes inapplicable, the scaled model facility at U.C. Berkeley will be used to investigate the problems brought out in this section.

6.3.6 Measurement of the Electrical Parameters of Returned Lunar Samples

It is proposed that some rock samples returned from the moon via missions prior to Apollo 19 be provided for laboratory measurement of electrical conductivity, dielectric permittivity, and magnetic susceptibility. The measurements of conductivity and dielectric permittivity are to be made on lunar rocks in their natural state and then subsequently subjected to various percentages of water saturation. Temperature will be a variable in addition to frequency, which will range from 10^2 Hz to 10^8 Hz.

Knowledge of the dispersion and absolute values of the reflection coefficient is essential to experiment design,as earlier comment has revealed. In particular, the spectra of reflections depends upon these parameters.

6.3.7 Scaled Model Simulation of Antennas

As verification of the broad validity of theoretical calculations of antenna gain, bandwidth, impedance, and radiation pattern, scaled model experimentation is required. The CSM and the antennas are to scaled down to a size convenient for mounting at an antenna site to be selected. A test antenna is to be erected at the same test site. The heights and separation of the Sounder and test antennas are to be selected so that the effect of the ground echoes will not invalidate the measurements.

Redundancy in methods of antenna calibration is essential to ensure that no gross errors are being made. The accuracy of the theoretical calculations may well-surpass that of the scaled model experiments.

6.3.8 Prototype Test

Prior to mission launch, ground and airborne tests of the prototype Sounder System are recommended as a means of total system and concept checkout. This safety precaution series of tests should be conducted over terrains for which good electrical description is available and for which lunar conditions are approximated. Glaciers become an obvious test target provided they have been electromagnetically sounded previously.

6.3.9 Development of Interpretation Software

Certain computer software is required for converting the raw Sounder data to maps of complex reflection coefficient, pulse delay, pulse distortion, apparent conductivity, apparent dielectric constant, depth of layering, probable occurrence of water, locations of inhomogeneities, etc. Three steps are visualized in this process, as follows:

1) data retrieval
2) data presentation
3) data interpretation.

The software for this modular processing must be developed well in advance of the experiment so that (a) optional experiment sequences may be initiated during or before the mission to enhance the scientific yield of the experiment, (b) data may be disseminated in meaningful form within the time window permitted for such activities, (c) to warn of any potential problem areas in data processing and permit their rectification prior to launch.

6.3.10 Variation of Antenna Calibration

Due to temperature changes, mechanical and thermal deflections of the antennas, and the possible antenna plasma sheath, an investigation should be initiated for a means of intermittent measurement of antenna impedance during the operation of the experiment.

6.3.11 Milestones

Milestones for funding and achievement of the objectives of the recommendations of Section 6.0 need to be developed. Some recommendations require immediate attention while others may be deferred or spread over a long time interval. Preparation of study task and funding milestones has not been an objective of this report.

Acknowledgments

Preparation of this report has been based upon the author's analysis of the experiment starting in January 1968, but especially since the start of Contract NAS2-4996 in June 1968. In the time since the initiation of the study, the author has benefited from discussions with the following:

Walter E. Brown	Jet Propulsion Laboratory
George R. Jr:acek	University of California, Berkeley
William I. Linlor	NASA-Ames Research Center
Roger J. Phillips	Jet Propulsion Laboratory
Leonard J. Porcello	University of Michigan

The author has particular appreciation for the counsel of Dr. Linlor who has monitored this contract since its inception. Dr. Roger Phillips has critically reviewed the manuscript and made many valuable suggestions and contributions concerning its scope and content and the validity of the science included.

REFERENCES

P. Beckman and A. Spizzichino, *The Scattering of Electromagnetic Waves from Rough Surfaces*, (Macmillian, New York, 1963).

J. J. Brandstatter, *An Introduction to Waves, Rays, and Radiation in Plasma Media*, (McGraw Hill Book Co., New York, 1963).

W. M. Brown and L. J. Porcello, "An Introduction to Synthetic-Aperture Radar," *IEEE Spectrum*, *6*, (9), pp. 52-62 (1969).

A. A. Burns, *On the Wavelength Dependence of Radar Echoes from the Moon*, Radio Physics Laboratory, Stanford Research Institute, Tech. Report (1969a).

A. A. Burns, *The Diffuse Component of Lunar Radar Echoes*,Radio Physics Laboratory, Stanford Research Institute, Tech. Report (1969b).

W. J. Burtis and W. I. Linlor, "Measurement of Lunar Surface Sheath," Space Sciences Laboratory, manuscript in preparation.

A. Dey, H. F. Morrison, and S. H. Ward, *Electric Fields from a Horizontal Electric Dipole Situated Above a Layered Lunar Half-Space*, University of California, Berkeley, Final Report, NASA Contract NAS 2-5078, Item 326, Space Sciences Laboratory Series 11, Issue 3.

V. R. Eshleman, "Radar Astronomy," *Science, 158*,3801, pp. 585-597 (1967).

B. D. Fuller and S. H. Ward, "Linear System Description of the Electrical Parameters of Rocks," *IEEE Transactions of Geoscience Electronics, GE-8* (1), pp. 7-18 (1970).

W. D. Grobman and J. L. Blank, "Electrostatic Potential Distribution of the Sunlit Lunar Surface," *J. Geophys. Res.*, *74*,16, 3943 (1969).

H. Heffner, "The Potential and Electric Field at the Surface of the Moon," *Tycho Study Group* (1965).

G. Hohmann, "Electromagnetic Scattering by Two-Dimensional Inhomogeneities in a Conductive Half-Space," manuscript in preparation (1970).

H. T. Howard, personal communication (1970).

G. R. Jiracek and S. H. Ward, *Oblique Electromagnetic Reflection from Layered Lunar Models*, University of California, Berkeley, Tech. Report, NASA Contract NAS 2-5078, Space Sciences Laboratory, Series 11, Issue 7 (1970).

Z. Kopal, *An Introduction to the Study of the Moon,* (Gordon and Breach, Science Publishers, New York, 1966).

J. R. Parry, *Integral Equation Formulations of Scattering from Two-Dimensional Inhomogeneities in a Conductive Earth,* Ph.D. Thesis, University of California, Berkeley (1969).

H. Petscheck, "Surface Electric Field Measurements," NASA 1965 Summer Conference on Lunar Exploration and Science, Falmouth, Massachusetts (1965).

R. J. Phillips and H. F. Morrison, *Lunar Sounding with Transient Electromagnetic Field,* University of California, Berkeley, Tech. Report, NASA Contract NAS 2-5078, Space Sciences Laboratory, Series 10,Issue 21(1969).

R. J. Phillips and S. H. Ward, "Alfven Wave Interaction with the Moon," manuscript submitted for publication (1970).

M. J. Rycroft, *Electrical Fields Near the Moon's Surface,* NASA-Ames Research Center, Moffett Field, California, Internal Report (1965).

W. W. Salisbury, personal communication (1967).

C. P. Sonett, D. S. Colburn, and R. G. Currie, *The Intrinsic Magnetic Field of the Moon,* Space Sciences Division, Ames Research Center, Moffett Field, California (1967).

W. Sullivan, "Radar to Help Trace Profile of Antarctica," *New York Times* (November 11, 1969).

G. L. Tyler, "Oblique-Scattering Radar Reflectivity of the Lunar Surface: Preliminary Results from Explorer XXXV," *J. Geophys. Res., 73,* (24), 7609-7620 (1968).

G. L. Tyler, personal communication (1969).

S. H. Ward, G. R. Jiracek, and W. I. Linlor, "Electromagnetic Reflection from a Plane-Layered Lunar Model," *J. Geophys. Res., 73,* (4), 1355, (1968).

S. H. Ward, G. R. Jiracek, and W. I. Linlor, "Some Factors Affecting Electromagnetic Detection of Lunar Subsurface Water," *IEEE Trans. Geoscience Electronics, GE-7,* (1), pp. 19-27 (1969).

APPENDIX I

Radar to Help Trace Profile of Antarctica

by
Walter Sullivan

Special to *The New York Times*; Cambridge, England, October 29, 1969

"In a series of 20 or more flights during the coming months, British scientists hope that, figuratively, they can peel back a large part of Antarctica's ice covering, disclosing the continent that lies beneath.

"They will use an airborne radar, mounted on a C-130 Hercules transport of the United States Navy based at McMurdo Sound. The equipment has already penetrated more than 14,800 feet of ice, recording a profile of the mountains and valleys underneath.

"It will be the first large-scale attempt at radar charting of the ice-buried continent surrounding the South Pole. The technique has been developed in recent years at the expense of three lives, one Russian and three British, lost when vehicles broke through snow bridges and fell down Antarctic crevasses.

"Altogether, at the request of the National Science Foundation in Washington, scientists at the Scott Polar Research Institute here have charted flight paths totaling 500 hours (roughly 50 missions).

"However, the need to install a new radar antenna on the Hercules has delayed delivery of the plane to Antarctica. Hence the number of missions that can be flown during the coming southern summer, which coincides with the northern winter, will probably be considerably less.

"The radar exploits the fact that radio waves of suitable frequency can penetrate ice (unless partially melted and hence electrically conducting). Ice-sounding radars have been

developed in the United States, the Soviet Union and at the Scott Polar Research Institute.

"When in 1964 the Russians first tried their system, which was carried across the ice by a vehicle with tracks it broke through a crevasse, killing the driver and seriously injuring two engineers.

"The next year the British, based at Halley Bay in Queen Maud Land, attempted to chart the buried land using the equipment designed here. Three men were lost as well as all scientific records from that journey and some from an earlier traverse.

"The airborne equipment to be used on the coming flights records the ice depths on 35 mm. film and, at the same time, displays the data so that the crew can make any needed adjustments. In this respect they believe the system is superior to the American one, which taperecords the data with no on-the-spot display.

"Airborne sounding represents a radical advance over past methods. The standard technique has been to set off explosive charges every few miles, recording the interval before the first echo returned from the rock far below. Only a few such soundings per day could be made, what with the hazards of over-ice tractor travel.

"Furthermore the record was not continuous and many features between explosion sites were unobserved. The radar method provides a continuous profile. The radar beam, in the suitable frequency range from 20 to 100 megahertz (megacycles), is very wide and hence additional echoes are obtained from surfaces not directly beneath the plane.

"This generates some rounding of the inscribed profiles, if the terrain is rough, but the distortion can be removed. A computer method to this end is being devised here. It has been

found that the radar measurements are generally as accurate as those made with explosions.

"A third method is to estimate depth from highly sensitive gravity measurements. These indicate how much low-density material (that is, ice) lies between the instrument and the rock below. This is quicker than explosion sounding, but less accurate.

"In preliminary tests more than 16,000 miles of Antarctic terrain have been scanned by radar. However it was found that any attempt at mapping would be futile unless accurate navigation was possible over the featureless ice sheet covering one of the largest and most rugged continents of the world.

"The new flight lines have been laid out to make possible navigational 'fixes' on an abandoned sno-cat here, a rock outcrop there, and other landmarks in the remote interior.

"The plane, on occasion, will refuel at such far-flung stations as the South Pole and Halley Bay, but will still be unable to cover the most distant zone of the continent.

"Ultimately the British hope they can be provided with a survey plane fitted with an inertial navigational system that will give them a continuous record of position.

"Although their equipment can penetrate more than two miles of ice, it did not strike bottom in parts of Marie Byrd Land. The specialists here believe this was because heat from within the earth has made the deep ice of that region soggy.

"There is evidence of latent or intermittent volcanic activity in Marie Byrd Land, and radar pulses would not be able to penetrate the soggy ice produced by such activity."

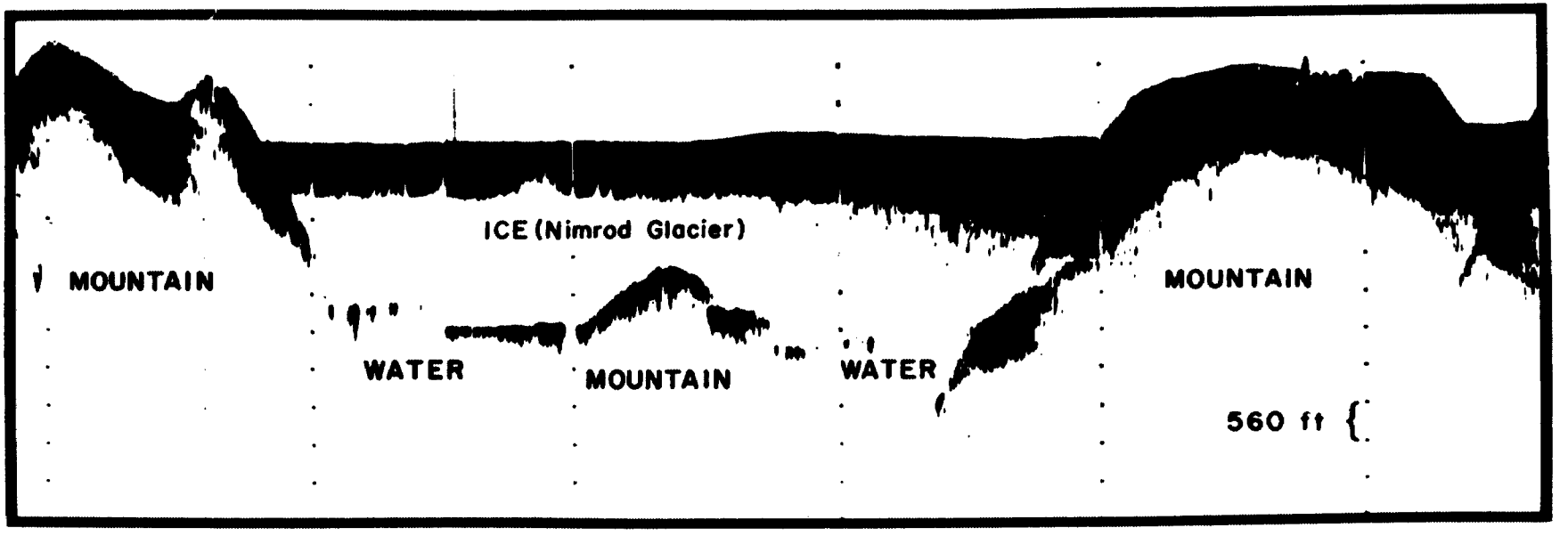
ICE (Nimrod Glacier)
MOUNTAIN
WATER
MOUNTAIN
WATER
MOUNTAIN
560 ft

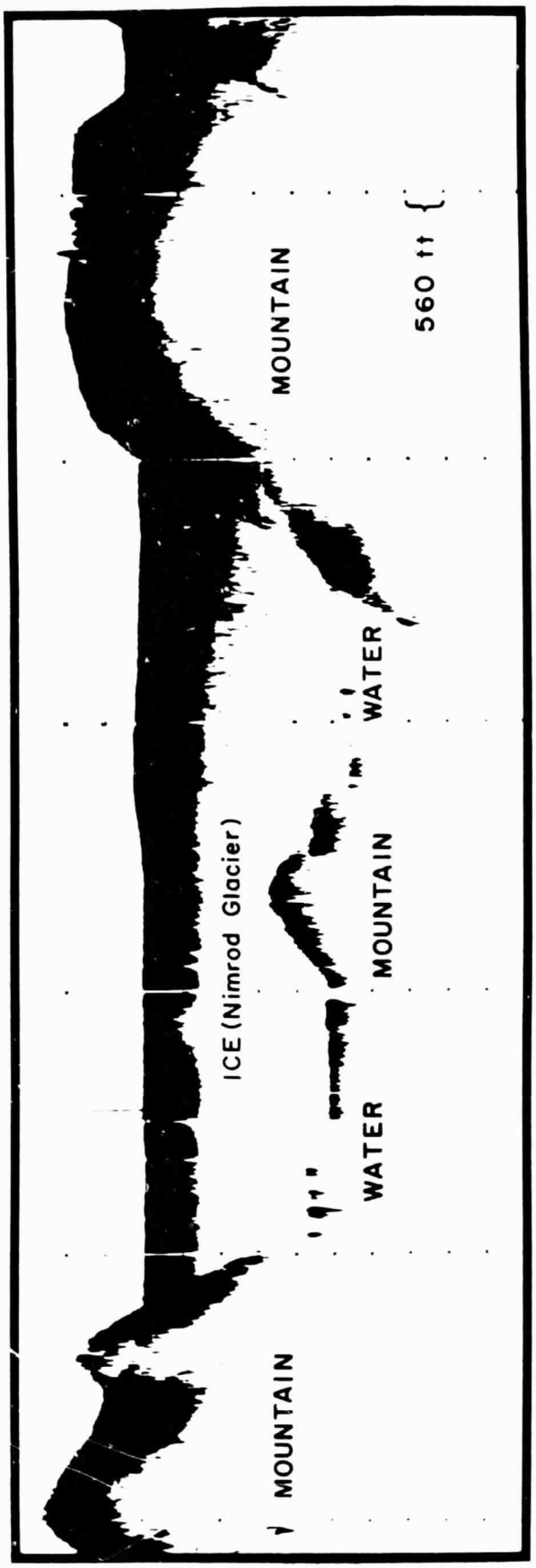
MOUNTAIN
ICE (Nimrod Glacier)
WATER
MOUNTAIN
WATER
MOUNTAIN
560 ft

APPENDIX II

Significance of the Lunar Electromagnetic Sounder Experiment

Some speculation is always inherent in assessing the potential significance of an experiment, and for this reason we have appended this discussion for this particular report.

The deep interior physical properties of the moon may be conveniently studied by three experimental concepts of the Apollo Lunar Orbital Science Program as follows:

1. gravity field data (S-band transponder)
2. magnetometry (orbital, Alsep)
3. Lunar Electromagnetic Sounder

and by two experimental concepts of the Apollo Lunar Surface Science Program as follows:

1. passive and active seismic
2. heat flow.

Gravity data have yielded the important discovery of mascons.

Orbital and lunar surface magnetometry has yet to provide any truly significant information on the electrical properties of the lunar interior. Further, no contribution from magnetometry can be expected at least until the following three parameters are measured simultaeously: lunar surface magnetic field, and the magnetic field, proton velocity, and proton density in the interplanetary medium upstream from the lunar surface (Phillips and Ward, 1970).

The seismic experiments of Apollo 11 and Apollo 12 have produced results that lead to a very fuzzy model of the lunar interior to depths of a kilometer or so. This fuzzy picture can be expected to clarify as more seismometers are placed on the lunar surface.

The potential significance of the heat flow experiment is good but the experiment has yet to be performed.

APPENDIX II

Significance of the Lunar Electromagnetic Sounder Experiment

Some speculation is always inherent in assessing the potential significance of an experiment, and for this reason we have appended this discussion for this particular report.

The deep interior physical properties of the moon may be conveniently studied by three experimental concepts of the Apollo Lunar Orbital Science Program as follows:

1. gravity field data (S-band transponder)
2. magnetometry (orbital, Alsep)
3. Lunar Electromagnetic Sounder

and by two experimental concepts of the Apollo Lunar Surface Science Program as follows:

1. passive and active seismic
2. heat flow.

Gravity data have yielded the important discovery of mascons.

Orbital and lunar surface magnetometry has yet to provide any truly significant information on the electrical properties of the lunar interior. Further, no contribution from magnetometry can be expected at least until the following three parameters are measured simultaeously: lunar surface magnetic field, and the magnetic field, proton velocity, and proton density in the interplanetary medium upstream from the lunar surface (Phillips and Ward, 1970).

The seismic experiments of Apollo 11 and Apollo 12 have produced results that lead to a very fuzzy model of the lunar interior to depths of a kilometer or so. This fuzzy picture can be expected to clarify as more seismometers are placed on the lunar surface.

The potential significance of the heat flow experiment is good but the experiment has yet to be performed.

We would therefore argue that another deep probing technique is essential to our understanding of the lunar interior and that the most likely candidate experiment is the Lunar Electromagnetic Sounder. It could readily clarify the fuzzy picture so far produced by the seismic experiments. Further, in a possibly dry inhomogeneous medium of the type suggested by the seismic experiments, electromagnetic techniques may reasonably be expected to return more useful information than do seismic methods.

Figure Captions

Figure 1. Conceptual sketch of antennas for Lunar Electromagnetic Sounder, deployed from Command and Service Module of Apollo spacecraft.

Figure 2. Detail of spacecraft and antennas deployed. The three-foot separation between spacecraft and antennas is nominal.

Figure 3. Sketch of field patterns expected from low-band dipole (240-foot tip-to-tip antenna).

Figure 4. Sketch of field patterns expected from high-band dipole (61.5-foot tip-to-tip antenna).

Figure 5. Estimated electron density distribution near lunar surface, Heffner "Overestimate Model" (after Burtis and Linor, 1970).

Figure 6. Sketch of a two-dimensional inhomogeneity beneath a topographic ridge (after Parry, 1969).

Figure 7. The horizontal secondary magnetic fields scattered from a ridge and from an inhomogeneity beneath a ridge (after Parry, 1969).

Figure 8. Schematic sketch of transmitted and received pulses for Lunar Electromagnetic Sounder.

Figure 9. Reflection from the lunar surface (1) and reflection from interface buried 1 km beneath the surface, for a box-car truncated continuous wave. Bandwidth of receiver not introduced.

Figure 10. Reflection from the lunar surface (1) and reflection from an interface buried 1 km beneath the surface, for box-car truncated continuous wave. Bandwidth of receiver 50 kHz.

Figure 11. Modulus of amplitude reflection coefficient versus frequency for typical wet and dry models of the moon (after Ward, et al., 1968).

Figure 12. Relative power reflectivity versus angle of incidence for bistatic reflection from the lunar surface (after Tyler, 1968).

Figure Captions (Cont'd)

Figure 13. Dielectric constant and permittivity function assumed for a gradational regolith (after Jiracek and Ward, 1970).

Figure 14. Computed amplitude reflection coefficient for a five-layered model of the moon that includes a gradational regolith. The apparent dielectric constant deduced therefrom pertains to the very top of the debris.

AAB219-2

CSM SOUNDER ANTENNAS

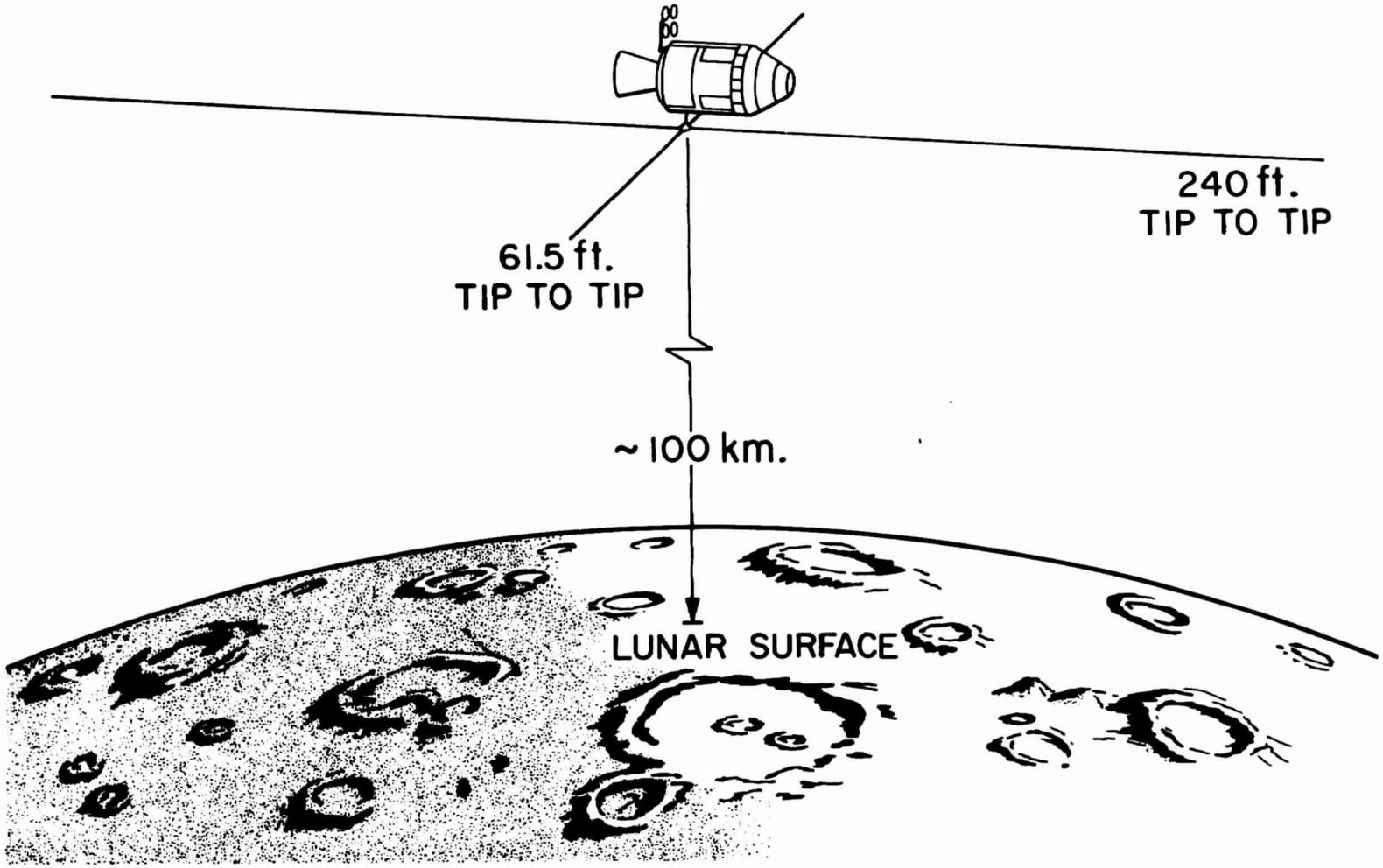

FIGURE 1

NATIONAL AERONAUTICS AND SPACE ADMINISTRATION
AMES RESEARCH CENTER MOFFETT FIELD CALIFORNIA

AAB219-1

COMMAND SERVICE MODULE WITH ANTENNAS DEPLOYED

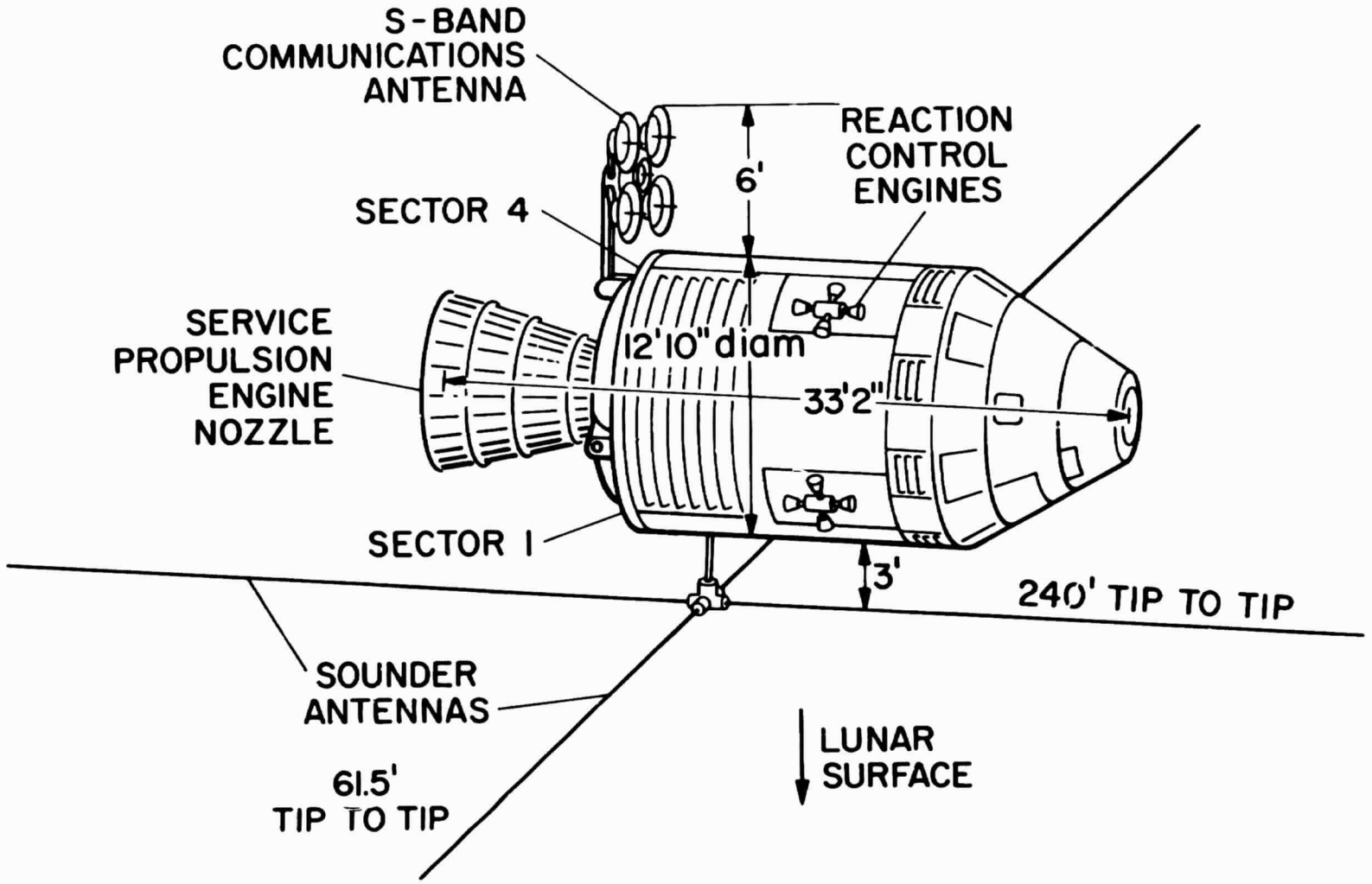

FIGURE 2

NATIONAL AERONAUTICS AND SPACE ADMINISTRATION
AMES RESEARCH CENTER MOFFETT FIELD CALIFORNIA

SOUNDER ANTENNA RADIATION PATTERNS

LOW BAND DIPOLE 0.1-5.0 MHz
(LONG DIPOLE)

FREQUENCY	ANTENNA LENGTH	RADIATION PATTERN
0.1 MHz	$\frac{L}{\lambda} = 0.02$ (SHORT DIPOLE)	
4.1 MHz	$\frac{L}{\lambda} = 1.00$	
5 MHz (CROSS-OVER FREQUENCY)	$\frac{L}{\lambda} = 1.25$	

$$E(\theta) = \frac{\cos\left(\frac{BL}{2}\cos\theta\right) - \cos\frac{BL}{2}}{\sin\theta}$$

FIGURE 3

SOUNDER ANTENNA RADIATION PATTERNS

HIGH BAND DIPOLE 5-0-20 MHz
(SHORT DIPOLE)

FREQUENCY	ANTENNA LENGTH	RADIATION PATTERN
5 MHz (CROSS OVER)	$\frac{L}{\lambda} = 0.3$ (SHORT DIPOLE)	
16 MHz	$\frac{L}{\lambda} = 1.00$	
20 MHz	$\frac{L}{\lambda} = 1.25$	

$$E(\theta) = \frac{\cos\left(\frac{\beta L}{2}\cos\theta\right) - \cos\frac{\beta L}{2}}{\sin\theta}$$

FIGURE 4

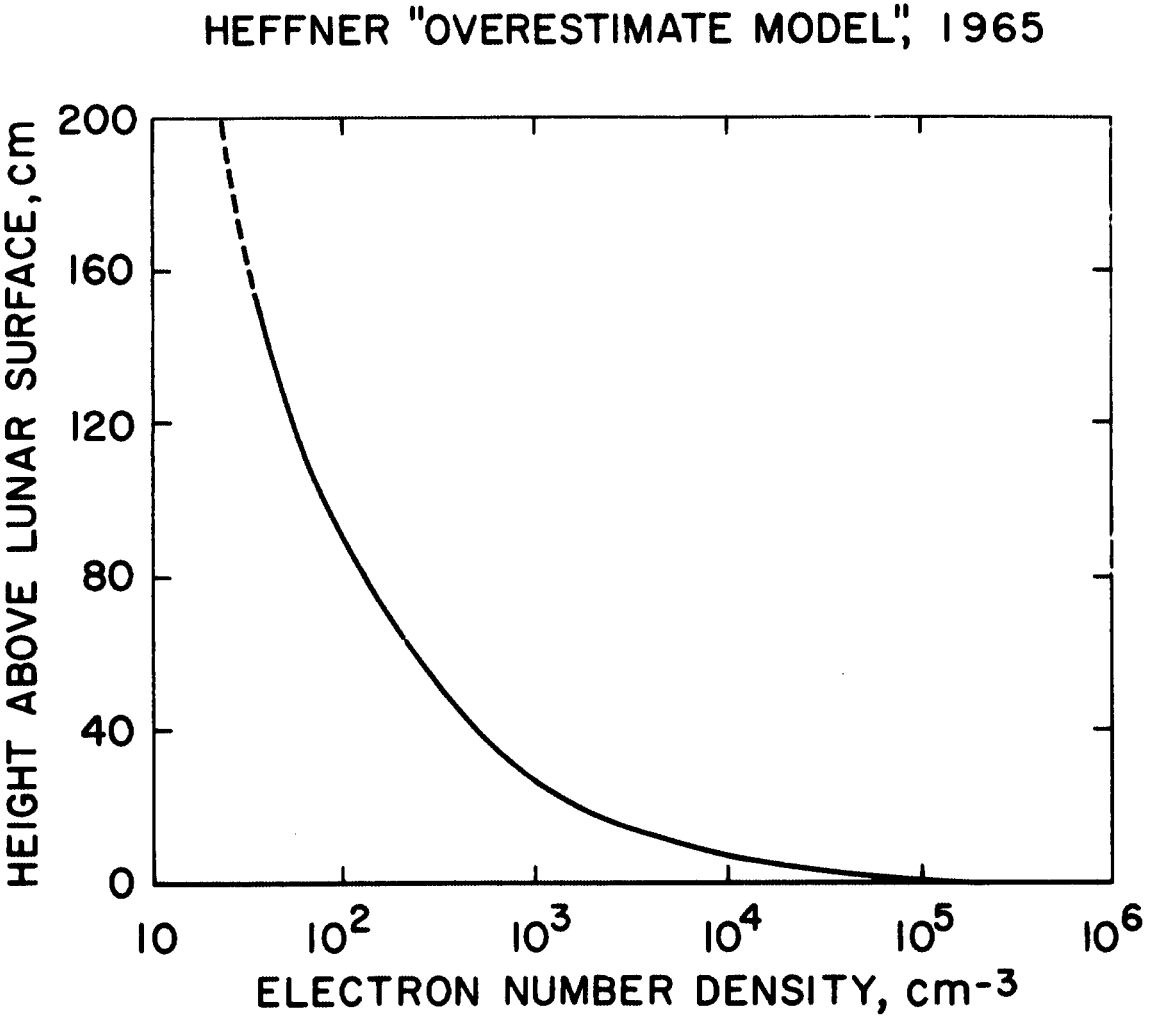

FIGURE 5

NATIONAL AERONAUTICS AND SPACE ADMINISTRATION
AMES RESEARCH CENTER, MOFFETT FIELD CALIFORNIA

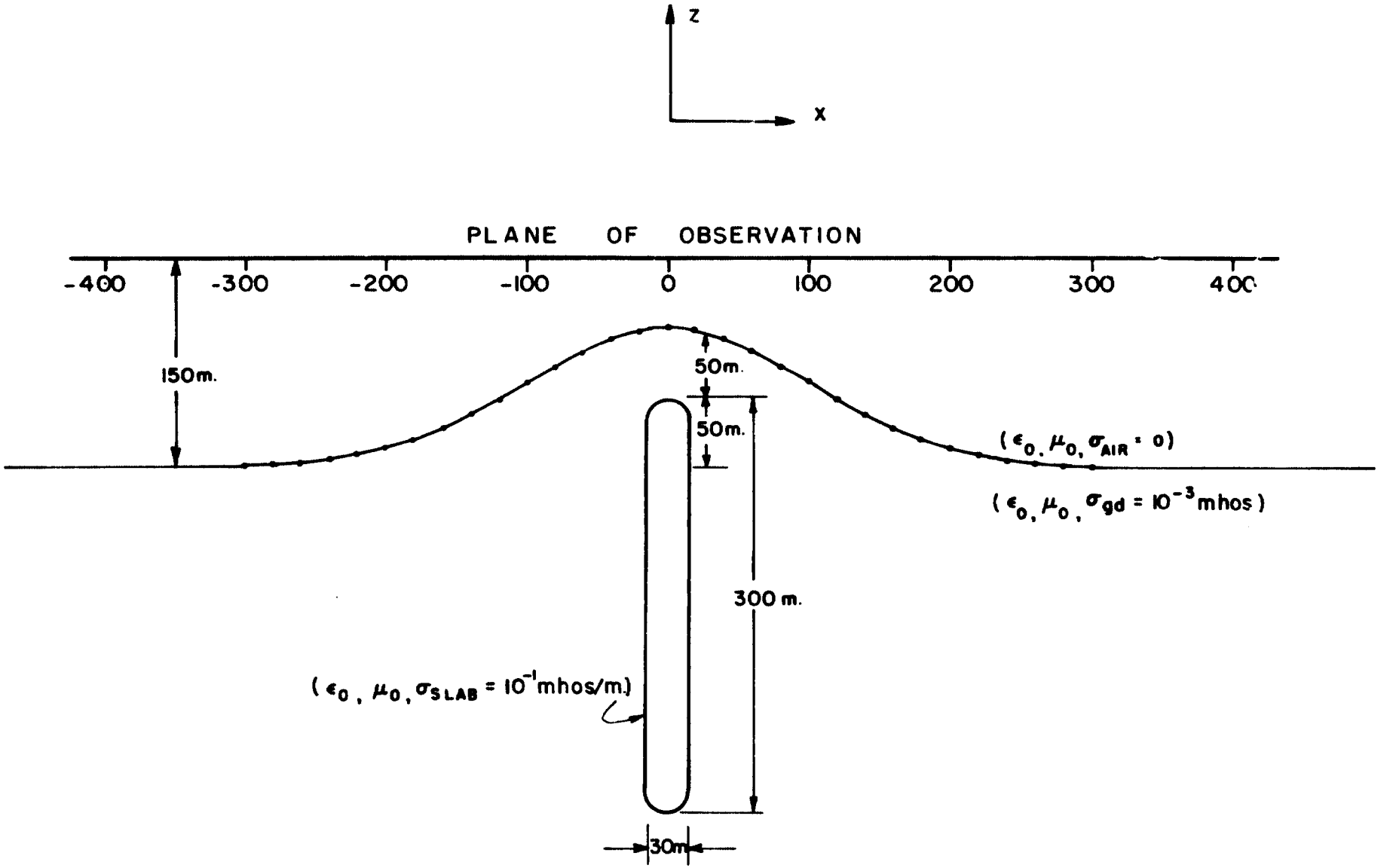
z
x
PLANE OF OBSERVATION
-400
-300
-200
-100
0
100
200
300
400
150m.
50m.
50m.
300 m.
30m
$(\epsilon_0, \mu_0, \sigma_{AIR} = 0)$
$(\epsilon_0, \mu_0, \sigma_{gd} = 10^{-3}\text{mhos})$
$(\epsilon_0, \mu_0, \sigma_{SLAB} = 10^{-1}\text{mhos/m})$

FIGURE 6

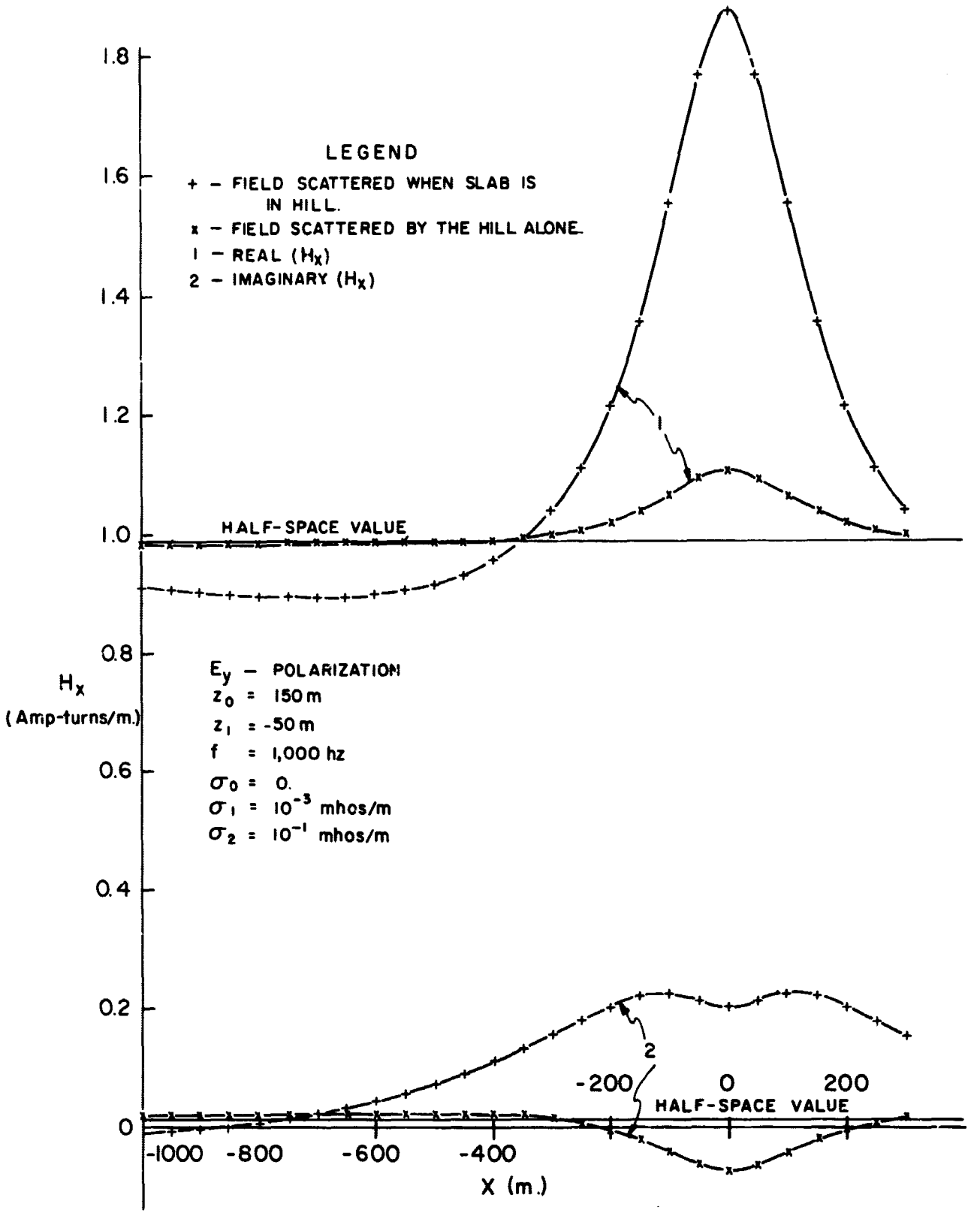
LEGEND
+ – FIELD SCATTERED WHEN SLAB IS IN HILL.
x – FIELD SCATTERED BY THE HILL ALONE.
1 – REAL (H_x)
2 – IMAGINARY (H_x)
HALF-SPACE VALUE
E_y – POLARIZATION
z_0 = 150 m
z_1 = -50 m
f = 1,000 hz
σ_0 = 0.
σ_1 = 10^{-3} mhos/m
σ_2 = 10^{-1} mhos/m
H_x
(Amp-turns/m.)
1.8
1.6
1.4
1.2
1.0
0.8
0.6
0.4
0.2
0
-1000
-800
-600
-400
-200
0
200
X (m.)
HALF-SPACE VALUE

FIGURE 7

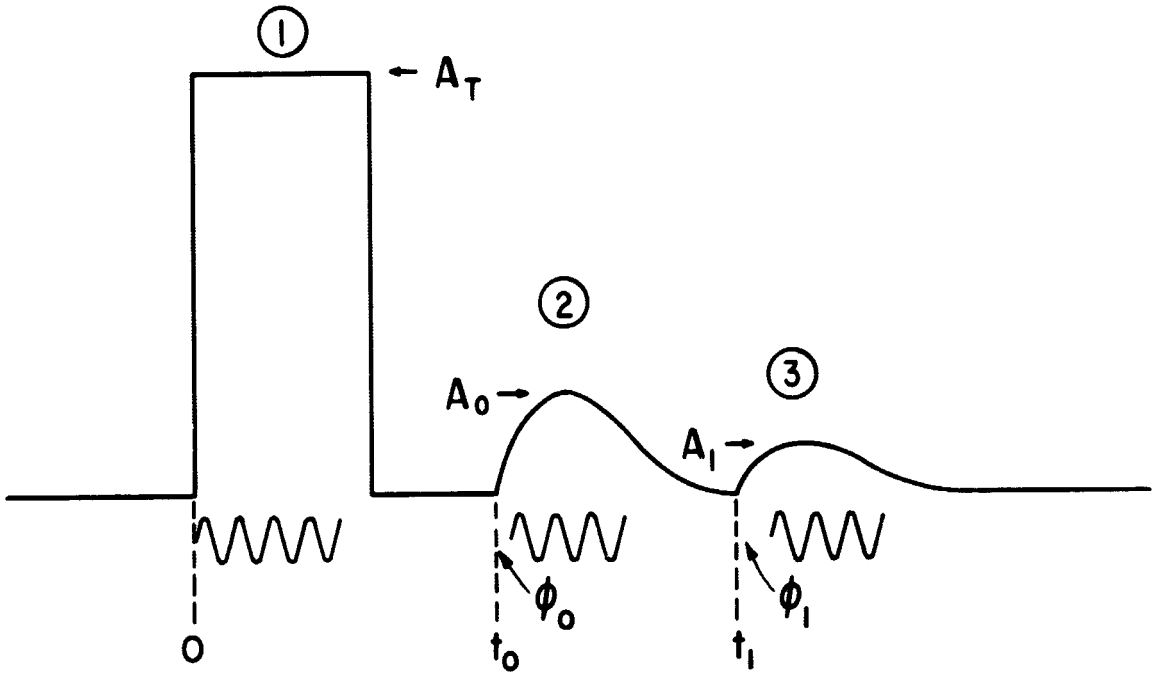

1. RECTIFIED ENVELOPE OF TRANSMITTED PULSE OF R F

2. RECTIFIED ENVELOPE OF PULSE RECEIVED FROM LUNAR SURFACE

3. RECTIFIED ENVELOPE OF PULSE RECEIVED FROM FIRST SUBSURFACE REFLECTOR.

FIGURE 8

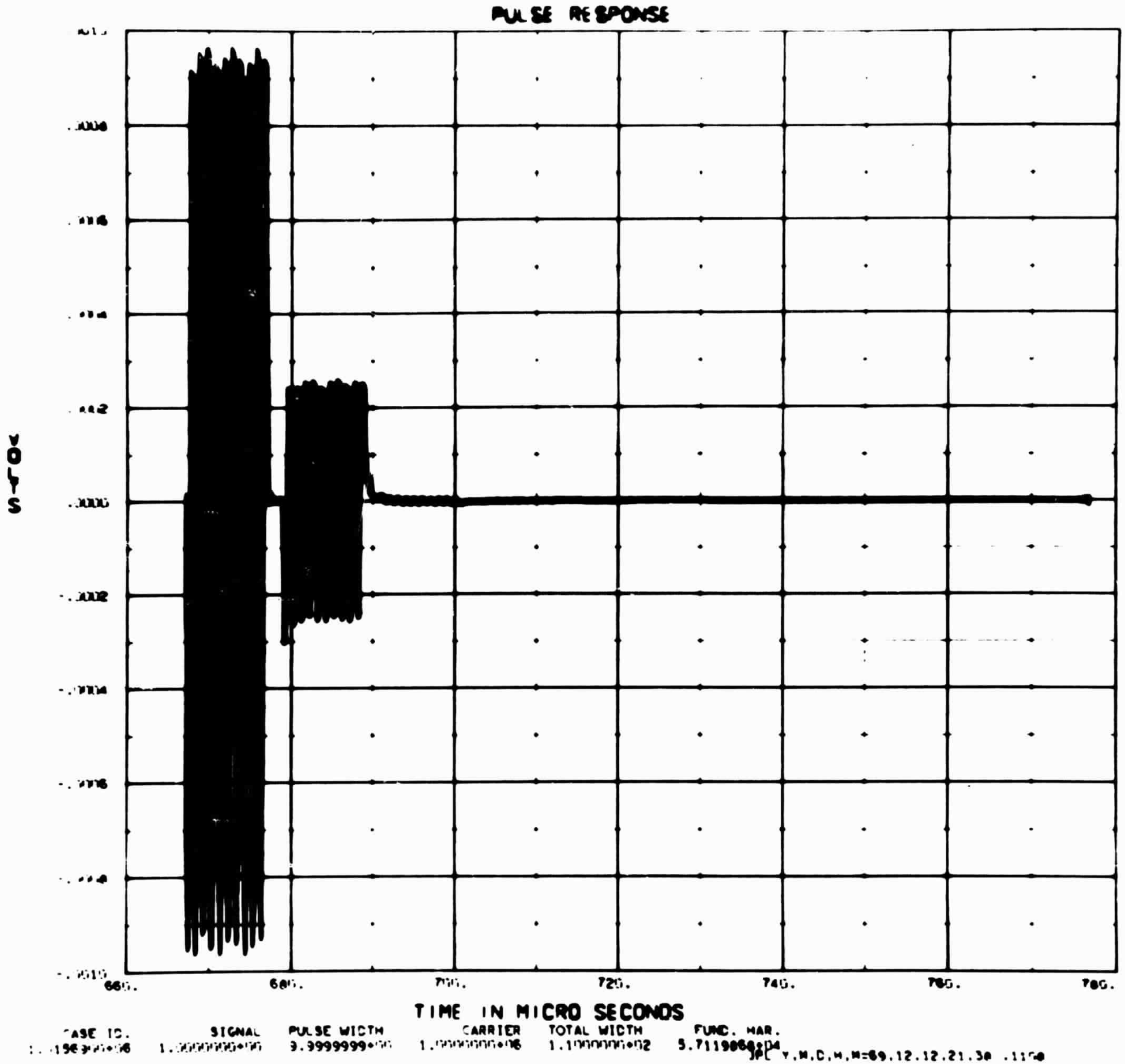
PULSE RESPONSE
VOLTS
TIME IN MICRO SECONDS
CASE ID.
SIGNAL
PULSE WIDTH
CARRIER
TOTAL WIDTH
FUNC. HAR.

Figure 9

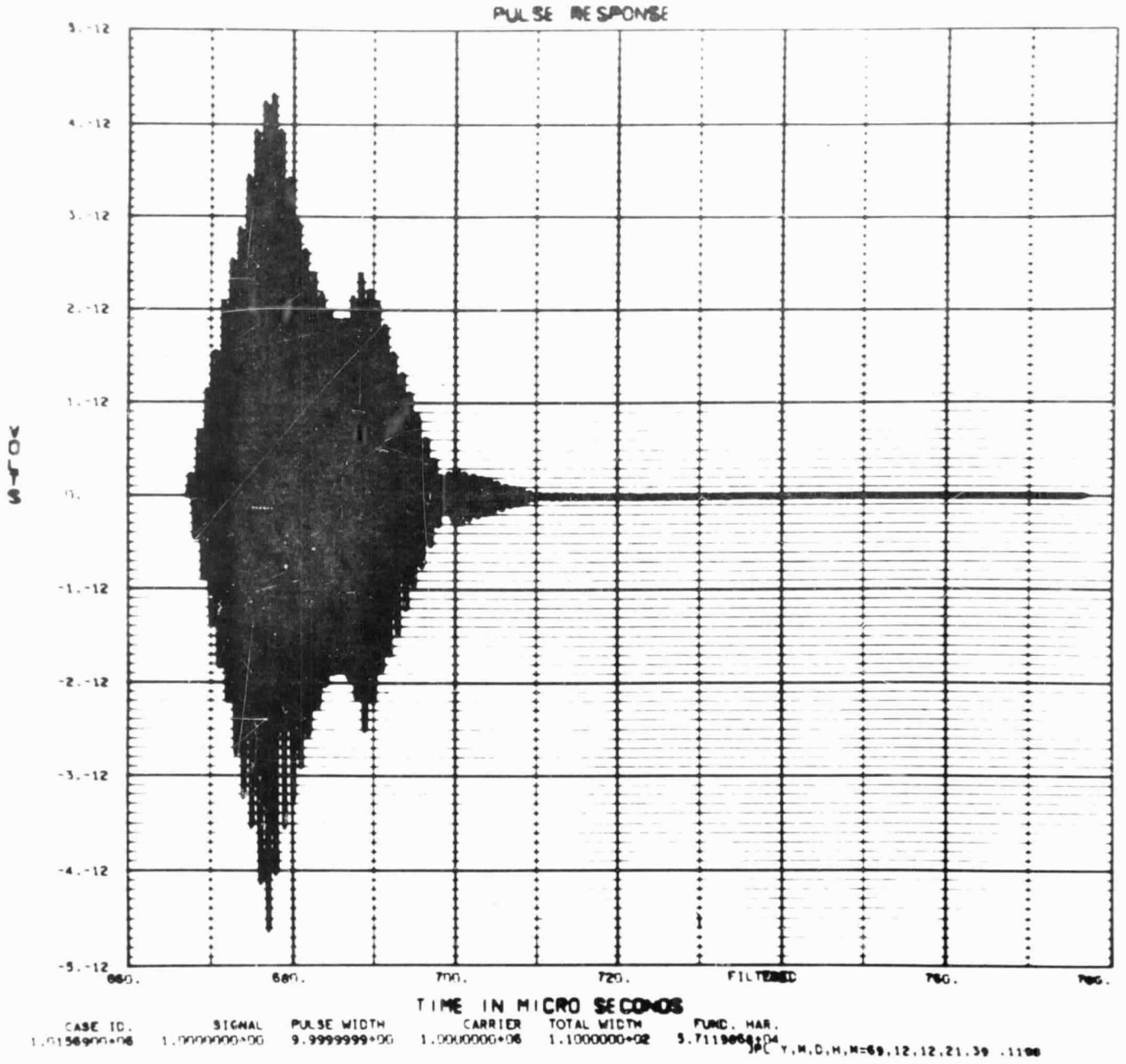
PULSE RESPONSE
5.-12
4.-12
3.-12
2.-12
1.-12
0.
-1.-12
-2.-12
-3.-12
-4.-12
-5.-12
VOLTS
660.
680.
700.
720.
740.
760.
TIME IN MICRO SECONDS
CASE ID.
SIGNAL
PULSE WIDTH
CARRIER
TOTAL WIDTH
FUNC. HAR.
1.0158000+06
1.0000000+00
9.9999999+00
1.0000000+06
1.1000000+02
5.7119068+04
Y,M,D,H,M=69,12,12,21,39 .1198

Figure 10

FREQUENCY VARIATION OF AMPLITUDE REFLECTION COEFFICIENT
(MODEL 2, WARD et. al., JGR 73, 1355, (1968))

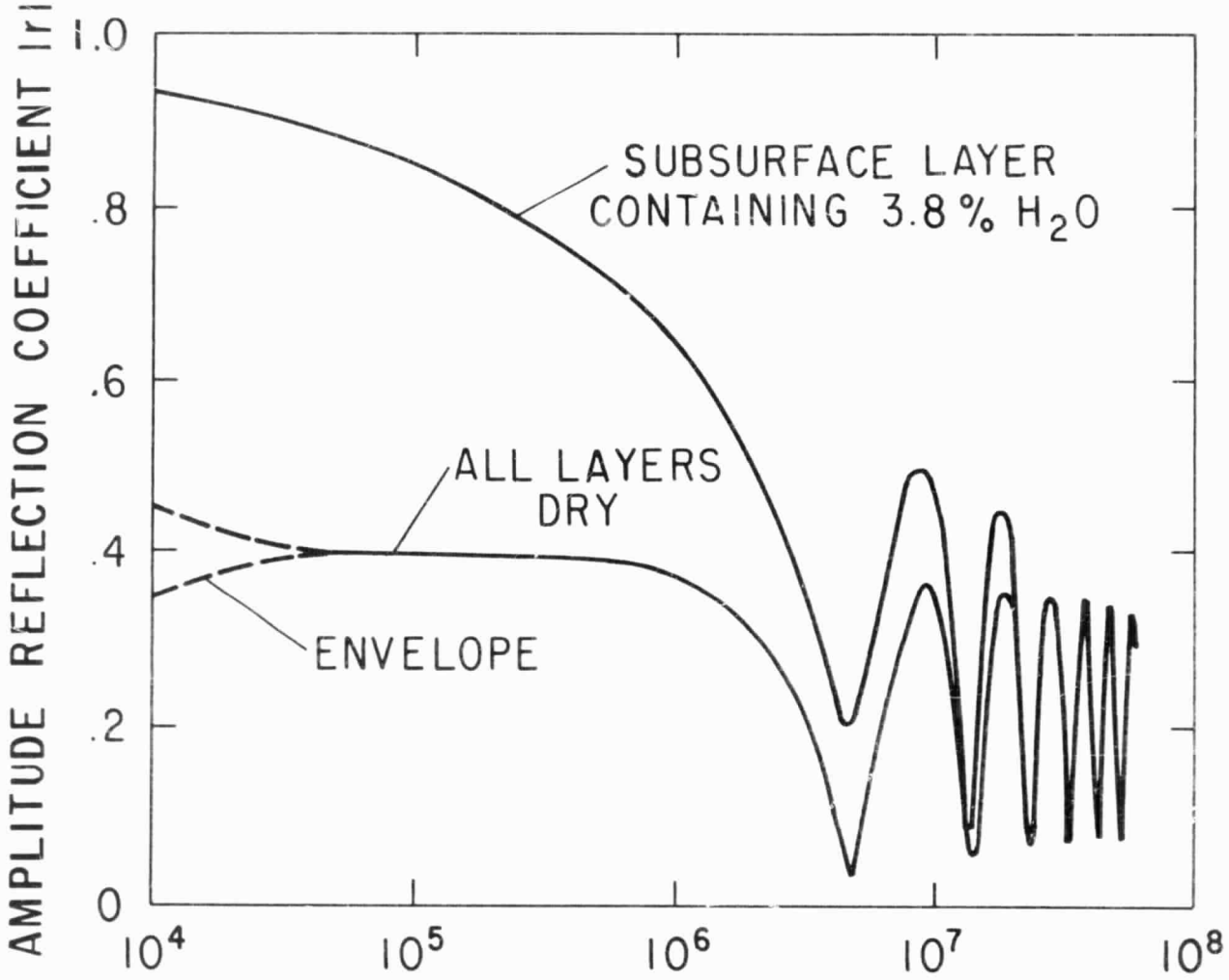

FIGURE 11

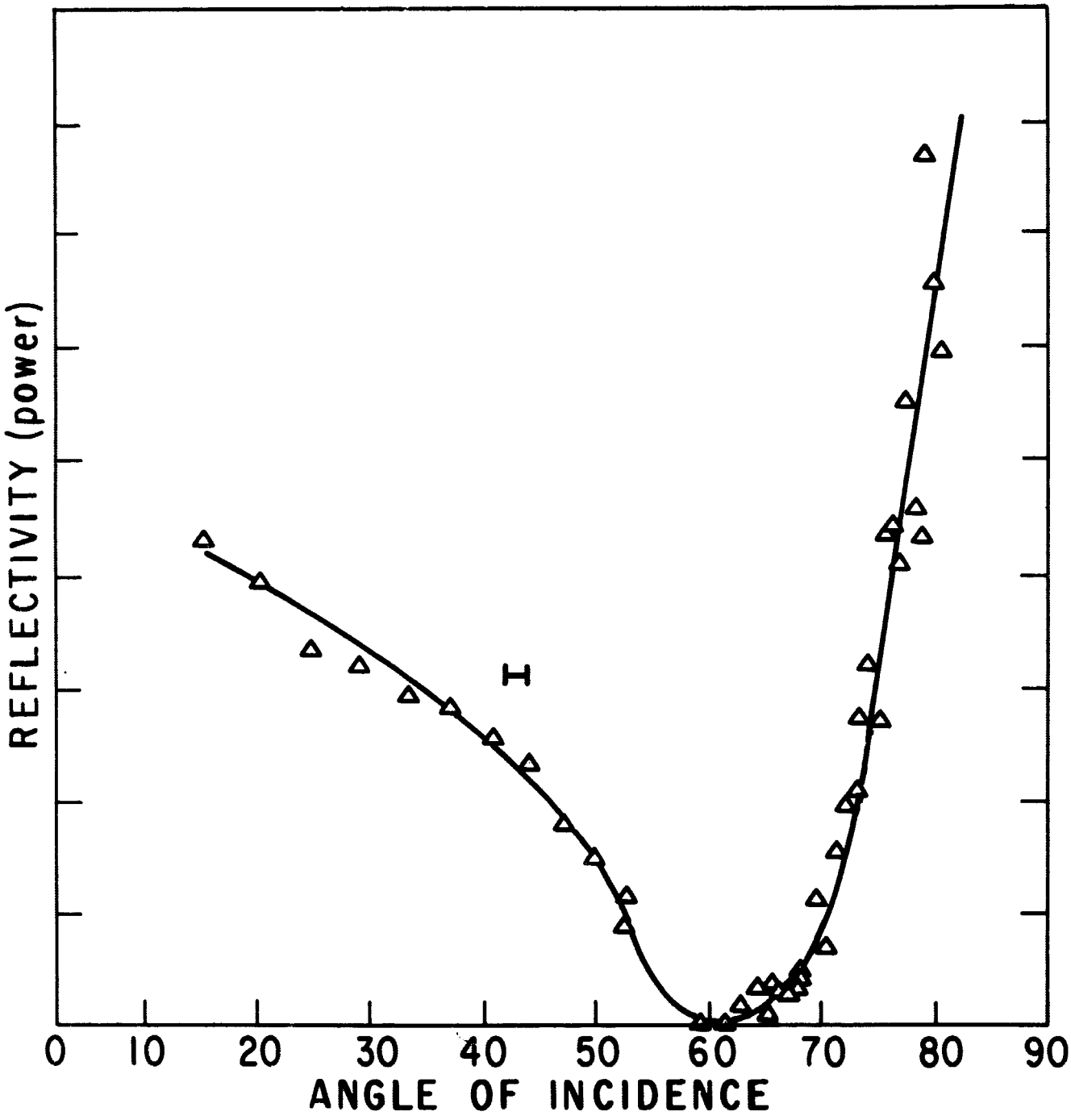
REFLECTIVITY (power)
H
0
10
20
30
40
50
60
70
80
90
ANGLE OF INCIDENCE

FIGURE 12

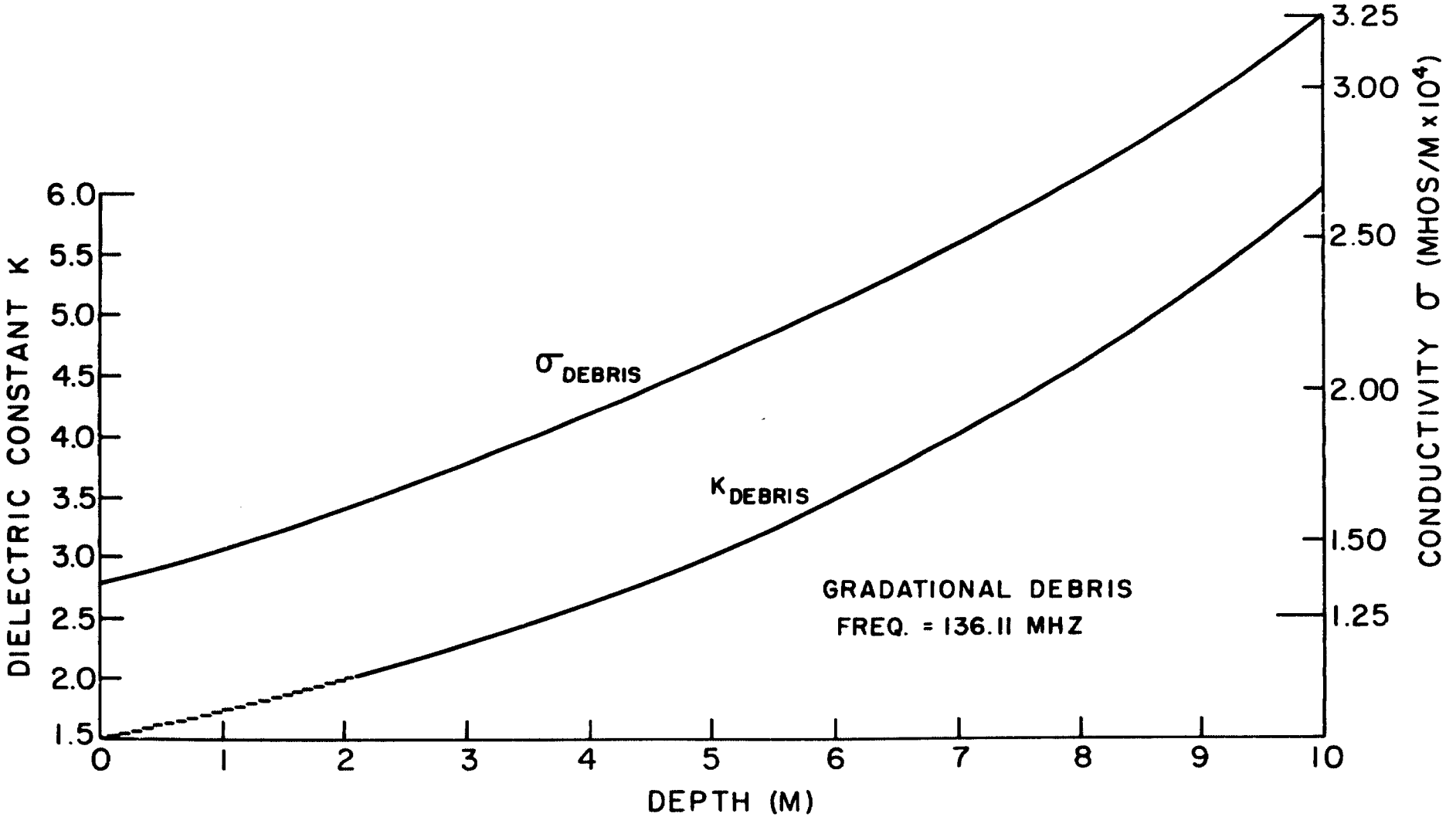
DIELECTRIC CONSTANT K
6.0
5.5
5.0
4.5
4.0
3.5
3.0
2.5
2.0
1.5
CONDUCTIVITY σ (MHOS/M x 10⁴)
3.25
3.00
2.50
2.00
1.50
1.25
σ DEBRIS
K DEBRIS
GRADATIONAL DEBRIS
FREQ. = 136.11 MHZ
0
1
2
3
4
5
6
7
8
9
10
DEPTH (M)

FIGURE 13

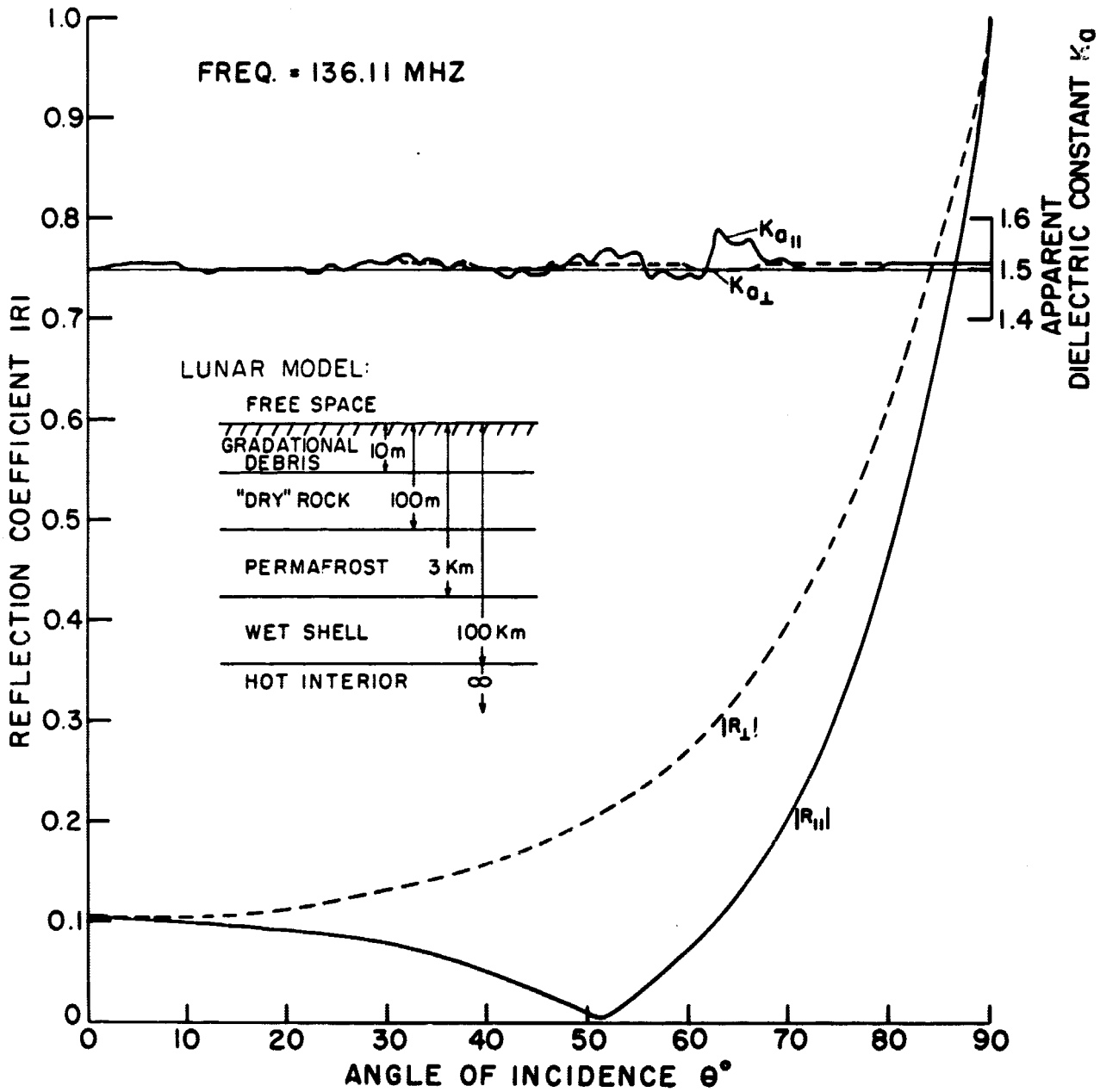
FREQ. = 136.11 MHZ
REFLECTION COEFFICIENT IRI
APPARENT DIELECTRIC CONSTANT Ka
ANGLE OF INCIDENCE θ°
Ka||
Ka⊥
1.6
1.5
1.4
|R⊥|
|R||
LUNAR MODEL:
FREE SPACE
GRADATIONAL DEBRIS
10m
"DRY" ROCK
100m
PERMAFROST
3 Km
WET SHELL
100 Km
HOT INTERIOR
∞
1.0
0.9
0.8
0.7
0.6
0.5
0.4
0.3
0.2
0.1
0
0
10
20
30
40
50
60
70
80
90

FIGURE 14